

## 6. APPLICATIONS TO REACTOR CONTAINMENT ANALYSIS\*

### 6.1. Introduction\*\*

Since the Three Mile Island accident, there has been a great deal of interest regarding the problem of hydrogen production, distribution, and combustion in LWRs. Regarding reactor safety analyses or studies, hydrogen combustion can involve wide time scales (between milliseconds in case of a detonation and several seconds in case of a slow deflagration) and pressures (between 4 and 30 times the initial pressure or more, depending on the reflections of the shock waves). These two parameters characterize the main combustion consequences of importance to reactor safety, i.e., pressure load and impulse (integral of pressure over time). In some cases, the temperature increase can also be of concern for the behaviour of equipment or the integrity of the containment, but, usually, this parameter presents no serious threat because the flame front travels comparatively fast because of propagation in structures. Depending on time and natural frequency scales, the effect of a combustion process inside containment can be divided in two main categories: static and dynamic loading. According to combustion propagation, this effect can be local (inside a compartment) or global (for the whole containment).

All the combustion modes are potentially possible for the same accident scenarios. The process of combustion during a severe accident is an ignition by a weak source, an electric spark, for example. Starting at low speed near the ignition point, the flame can be strongly accelerated by turbulence, and thus the flame speed can reach levels well above those of the speed of sound with complex systems of pressure waves. This combustion or acceleration process depends on many parameters, such as concentrations of reactants and diluents, presence and nature of ignition source, geometry, initial thermalhydraulics (temperature, pressure, and turbulence, etc.), and operating system effects (spray, venting, etc.).

First of all, to ensure the adequacy of developed criteria with the reactor safety requirements, the range of influencing parameters has to be specified for various severe accident scenarios and different geometry. Guidelines should be defined to apply the developed criteria to reactor scale.

#### 6.1.1 *General Data for Criteria Application*

The aim of this introduction is to summarize some general data related to our present knowledge of hydrogen behaviour in actual NPPs. This task has been done in order to avoid plant-specific considerations, especially for the guidelines to apply foreseen macro-criteria on FA and DDT, and also to be sure that the developed criteria are available for the whole range of severe accident scenarios and geometry configurations.

For safety reasons, the goal has to be a minimization of severe accident scenario occurrences dealing with accidental combustion and strong FA, which could jeopardize the containment integrity. The main parameters influencing the development of such a combustion process can be summarized in the areas of mixture concentration (including initial thermodynamics conditions) and geometrical configuration.

---

\* Dr. W. Breitung is the lead author of Chapter 6.

\*\* E. Studer contributed Sections 6.1 through 6.3.

Present criteria developed for FA and DDT entail these two different informations connected to mixture composition and geometrical configuration.

#### *6.1.1.1 Mixture composition*

Mixture composition is strongly affected by the initial thermalhydraulic conditions, i.e., the initial temperature and degree of initial turbulence. Initial temperature is of interest because the sensitivity of a given mixture increases with higher temperature (reaction rate, detonation cell size, less-efficient turbulence quenching). Concerning turbulence, the main effect can be considered as a balance between initial turbulence and flame-induced turbulence and mixing. The initial pressure is normally not relevant to the behaviour of a flame front, but it can be of importance for the value of absolute pressure obtained during a combustion process.

For mixture composition, the following parameters should be considered: mean values and gradients for combustible gases (hydrogen or carbon monoxide or both) and diluents (steam or carbon dioxide or both) and oxidant concentration. Any indication of gradients between a possible ignition position and the end of the combustion path is also important because in terms of negative combustible gradients, the combustion may be quenched during propagation. For this case, the effect should only be local (inside a compartment) and not global (for the whole containment). Consequently, the way to jeopardize the containment may be different: possible missiles created by a local explosion compared to global pressure loading of the containment.

Regarding the generation of combustible gases, many severe accident scenarios could be divided in 6 different phases; each scenario can only involve two or three phases or parts of these phases:

- Phase 1 : hydrogen release during in-vessel clad oxidation (main short-term source of hydrogen);
- Phase 2 : from molten pool formation to vessel lower head failure;
- Phase 3 : reflooding of degraded core;
- Phase 4 : long-term behaviour without core-concrete interaction;
- Phase 5 : short-term core-concrete interaction; and
- Phase 6 : long-term core-concrete interaction.

For each phase, the gaseous composition in the containment must be known in order to estimate or calculate the behaviour of potential combustion phenomena. Aside from the above 6 phases of hydrogen generation, the initial steam release phase prior to the hydrogen production can also have an important influence on the combustion regime because it affects the long-term distribution of heat sources and sinks, and hence the convection flows.

The mixture composition or the occurrence of ignition can also be influenced by the following system boundary conditions:

- pre-inertization in the containment as in some BWR power plants,
- recombiner mitigation devices as in a Belgian large dry PWR power plant,

- igniters as in some US nuclear power plants, and
- operating systems (spray, venting, etc).

In the following lumped-parameter application, scenarios related to phase 2 and recombiners will be examined.

#### 6.1.1.2 *Geometry*

The geometry of a combustion volume is the most important and the most complex parameter for FA. Especially, in case of real situations, geometry of a single combustion compartment and arrangement of a multi-compartment combustion process are of main importance. The three main parameters can be summarized as size of obstacles, distance between 2 obstacles, and degree of confinement (all geometrical discontinuities on the combustion path). In actual NPP geometry, data such as blockage ratio or spacing of obstacles cannot always be defined because of their complexity. The main characteristics of such geometry are the very irregular arrangements compared to well-defined experimental conditions. Long channels such as explosion tubes or those used in the RUT [6.1] or FLAME [6.2] facilities can be regarded as quasi-one-dimensional, but real geometry leads to two- or three-dimensional combustion processes. The main parameter in this case is the expansion flow created in the unburned mixture, which strongly depends on the degree of confinement. At the present time, experimental programs are not designed to get an appropriate model in all needed scenarios of this complex phenomenon.

## **6.2. Illustration of Combustion Calculation at Reactor-relevant Scale with Lumped-parameter Approach [6.3]**

Concerning the lumped- parameter approach, the whole methodology described in Chapter 5 could be applied on a simplified test case. The geometry chosen is that of a prototypic French 900 MWe PWR. The severe accident scenario is assumed to be a 2-inch small-break cold-leg loss-of-coolant accident (LOCA) with safety injection and spray failure. Containment transient has been calculated using the lumped-parameter code RALOC mod4.0 [6.4] using about 85 nodes in the gas phase of the containment. No mitigation measures are taken into account in this calculation, and hydrogen production during in-vessel core degradation is maximized. Hydrogen and steam distribution at the time of vessel failure is shown in the Figure 6.2-1.

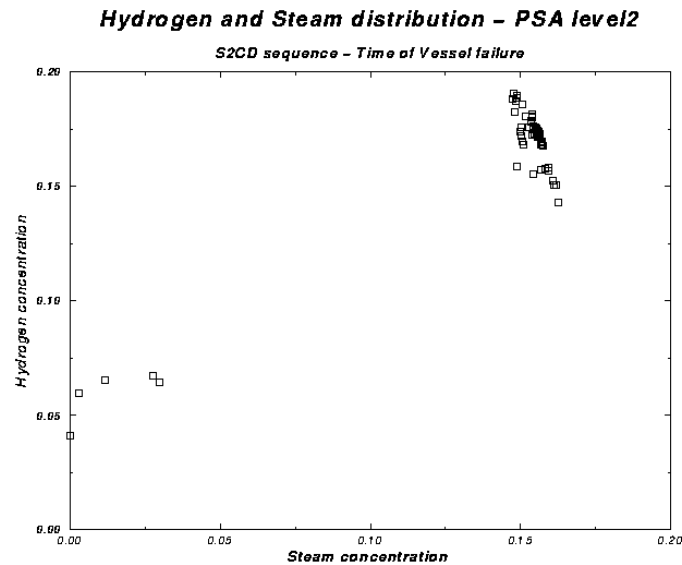


**Figure 6.2-1 Hydrogen and steam concentration in each control volume at vessel failure time (2-inch-diameter LOCA)**

Each point represents one gas node in the containment atmosphere. The mixture is quite homogeneous in the whole containment: hydrogen concentration is between 14 and 18 vol % and steam is around 14 to 16 vol %. Some rooms show special behaviour because they are poorly influenced by the main convection loops (basemat and in-core instrumentation room located in the lower part of the containment).

This hydrogen distribution has been used as an initial condition in the probabilistic safety analysis (PSA) 2 simplified combustion model. The geometry has been modified to ensure that the restrictions of the model are verified: this means, for example, that channel regions such as the annular region have been subdivided to create an arrangement of cubic volumes. The containment is now subdivided into about 500 rooms, with more than 1000 atmospheric junctions. Concerning modelling, an additional parameter has been introduced to enhance the vertical flame propagation of upward direction versus horizontal or downward direction. This is done by using a simple parameter  $K$  ( $>1$ ) to weight each atmospheric junction:  $K$  is applied to upward vertical junction, 1.0 to horizontal junction, and  $1/K$  to downward propagation. Concerning ignition, studies have shown that potential ignition locations are located in the lower part of the containment (between  $-3.5$  and  $4.65$  m). Three test cases have been simulated with our model:

- Case 1: ignition in the annular region (level 0.0 m) loop number one (all the rooms involving components of the first reactor primary circuit loop) with  $K = 1.0$ ;
- Case 2: same as case 1, but  $K = 5.0$ ; and
- Case 3: ignition in the residual heat removal system exchanger room (level  $-3.5$  m) with  $K = 1$ .

Results are given in Figure 6.2-2 in terms of flame velocity  $V_F$  in metres per second for the 3 test cases and for loop number one (the mixture in room number R448 is non-flammable). Geometry has been averaged on the initial geometrical arrangement used for distribution calculation.

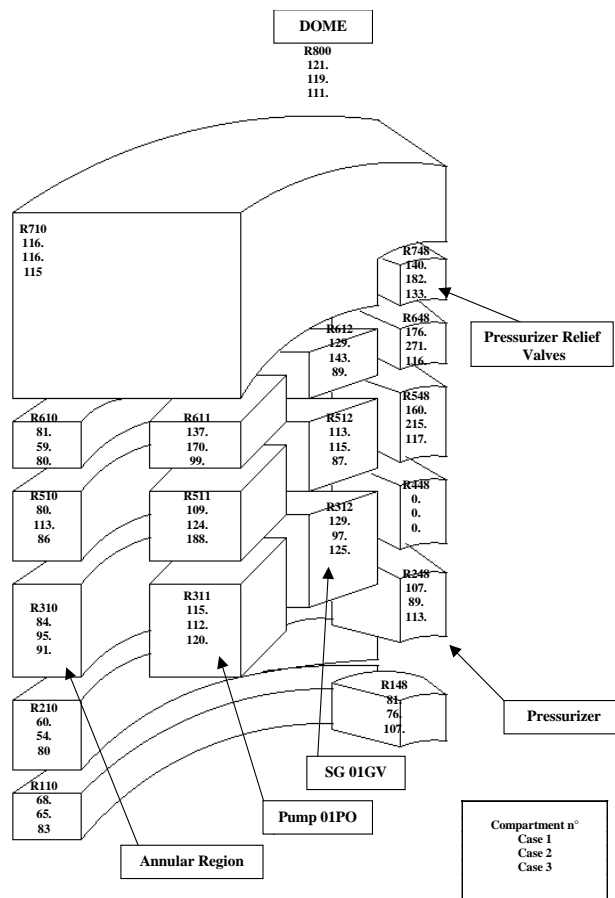


**Figure 6.2-2 Turbulent combustion velocity in each control volume (2-inch-diameter LOCA at vessel failure time)**

In the dome region, the flame velocity is less than 120 m/s. Combustion velocity is slow in the lower part of the containment. Acceleration can be seen in the steam generator, pump or pressurizer rooms (mainly for the second test case where the vertical upward combustion is enhanced). This implies, for example, that the dome region burns before the lower part of the containment is ignited. Maximum flame velocity is about 270 m/s in the upper part of the pressurizer rooms. If one looks at the other loops, the results are the same, and a maximum flame velocity of 430 m/s is calculated in the upper part of the pump region on loop number 3. One important phenomenon, which is not modelled in the present combustion process, is the occurrence of multiple ignition in a single room if the combustion process arrives from 2 or 3 different room connections at the same time.

Our simplified modelling for this hydrogen distribution test case (which can represent an upper bound for hydrogen distribution) does not predict any dynamic effect on the containment (fast turbulent deflagration, DDT or stable detonation) although the hydrogen mixture is very sensitive. Large open sections between volumes in a French 900 MWe PWR reduce the FA process. This study has only been performed to have an estimation of the FA process in a real containment geometry. These conclusions must be treated as preliminary because of the simplification in the modelling and the lack of knowledge concerning flame propagation in real 3D geometry.

## 6.3 Lumped-parameter Approach

This section is dedicated to application of criteria developed in Chapter 3 (criteria for FA and DDT). The example given here is related to the lumped-parameter approach for containment thermalhydraulics calculations. Examples for multi-dimensional CFD tools are given in the next section. Lumped-parameter nodalization is important because in many countries and for several years, lumped-parameter codes are often used for hydrogen risk analyses in the containment. Thus the database for hydrogen distribution covers a wide spectrum of postulated severe accident scenarios.

The criteria developed in Chapter 3 are expressed in terms of necessary conditions. They can be applied to select in a large number of possible scenarios that are important for FA or DDT. Then for these scenarios, detailed distribution and combustion calculations should be performed with detailed modelling (CFD models) in order to quantify loads to the third barrier (containment) and then structural mechanics behaviour.

### 6.3.1 Criteria

The following 3 criteria were developed in Chapter 3:

- the necessary condition for detonation propagation (criterion 1),
- the necessary condition for DDT (criterion 2) and
- the necessary condition for flame acceleration (criterion 3)

In the present study, criteria 1 and 2 will be aggregated and expressed in the following application by the  $L/\lambda$  criterion.

Criterion 2 is divided in 2 parts:

- requirements for DDT in terms of fast flame, critical flame, or shock Mach number. This part will not be studied because one needs to calculate the propagation of turbulent flames in a lumped-parameter approach. Therefore, simplified models like the one described in the previous section can be used. The present study aims only to use distribution results for estimating the potential for FA or DDT.
- onset of DDT: the  $7\lambda$  criterion. Regarding the lumped-parameter approach, this criterion is expressed in terms of size of a room or block of rooms. The key point is to define this geometrical size, and some possible rules are given in Chapter 3. This criterion should not be applied in case of strong hydrogen gradients (near the break if the release velocity is high compared with the convection velocity).

Criterion 3 is expressed in Chapter 3 by two different critical values depending on  $\beta(Le-1)$ . To avoid uncertainties in the value of activation energy  $E_a$ , it has been proposed to use a temperature-dependent  $\sigma$ -value  $\sigma^*(T_w)$  despite the preceding critical values (Figure 3.2.3-1). This is considered valid for a hydrogen-air-steam mixture without any others diluents, which is the foreseen mixture encountered in the containment during a severe accident scenario. It has been chosen to express criteria by the 2 manners, and to compare the results in the following application. This criterion is expressed by the  $\sigma$ -criterion in the following application.

### 6.3.2 Values Used to Calculate the Criteria

Regarding lumped-parameter calculations, the following variables are calculated in each control volume at each time step: total pressure  $P$ , gas temperature  $T$ , gas composition (mass or volume fractions of each gaseous species).

Geometrical data affect the total free volume of the cell  $V_{ii}$ , the height  $H_i$ , the sump area  $S_{pi}$ , the total wall area  $S_{wi}$  and the area of gaseous flow path between « cells »  $S_{ij}$  (Figure 6.3.2-1).

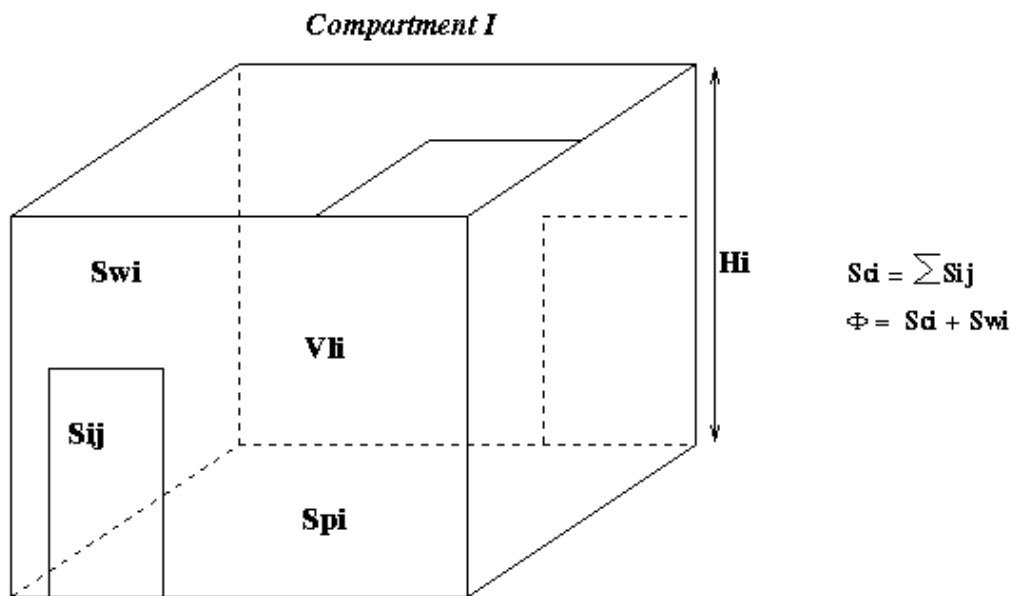


**Figure 6.3.2-1 Compartment geometrical parameters in lumped-parameter approach**

#### 6.3.2.1 Detonation cell size

A correlation proposed by S. Dorofeev, (see Appendix D of this report) can be used to determine the  $\lambda$  criterion. The detonation cell size is the result of the fitted function depending on initial pressure, temperature, steam, and hydrogen concentrations.

#### 6.3.2.2 Characteristic size $L$ of the room

The following guidelines have been derived in Chapter 3:

- For a cubic single room,  $L$  corresponds to the height of the room,
- For a single room where the width ( $W$ ) is smaller than the length ( $D$ ) and the height ( $H$ ):  
 $L = (D + H)/2$
- For two connected rooms:  $L = L_1 + \alpha \times L_2$  where  $\alpha = (1 - BR)^{1/2}$ ;  $BR$  represents the blockage ratio between the two rooms; this means the open area versus the total area. If the  $BR$  is smaller than a

critical value (0.1 for example), the two interconnected rooms are considered as a single one using the preceding formula to determine  $L$ .

- For a system of interconnected rooms,  $L = L_1 + \alpha_2 \times L_2 + \alpha_3 \times L_3 \dots$   $\alpha_i$  are calculated using the preceding definition. If it is difficult to define a BR in a real containment, then alternative definitions such as  $(L_1 \times S_{1i}/V_1)^{1/2}$  or  $(6 \times S_{1i}/(S_{wi} + S_{ci}))^{1/2}$  may be used.

The preceding rules have a clear definition with cubic volumes, comparable sizes, and small connecting flow paths. Unfortunately, in a large dry French-type PWR, the "room" volumes are not always cubic, the atmospheric junction areas are very large, and two interconnected volumes can have very different characteristic sizes.

There are different ways of calculating the characteristic size  $L$ . The first one is to look at the drawings of the NPP containment and to define a characteristic length scale for each room as long as it is possible to define a room. Then, rules defined above can be applied. A second possibility is to use a nodalization scheme (control volumes) built for a lumped-parameter analysis of hydrogen distribution with a lumped-parameter code. Using this second approach, the rules defined above lead to unrealistic characteristic length mainly because in the nodalization the control volumes are not always "rooms" but free volumes with large openings. Because of this fact, a special set of rules has been developed for a 900 MWe French PWR (see Appendix F). Sensitivity studies of the different nodalization schemes of the same containment have not been performed.

### 6.3.2.3 *Other mixture characteristics*

Others parameters of mixture characteristics are necessary to express the  $\sigma$  criteria. These are

- $\sigma$ : density ratio between fresh ( $\rho_u$ ) and burnt ( $\rho_b$ ) gases;
- $T_b$ : temperature of the burnt gases;
- $Le = \lambda/(\rho \times C_p \times D)$ : Lewis number with  $\lambda$  the thermal conductivity,  $\rho$  the density,  $C_p$  the heat capacity of the gaseous mixture (at initial temperature), and  $D$  the diffusion coefficient of the limiting gaseous species;
- $\beta = E_a(T_b - T_u) / (R \times T_b^2)$ : Zel'dovich number with  $E_a/R$  the reduced activation energy.

Fourth-order polynomial regressions are used to calculate the heat capacity  $C_p(T)$  of each chemical species. To simplify,  $T_b$  is calculated assuming a complete combustion at constant pressure. The mixtures studied are relatively lean equivalent hydrogen-air mixtures (dry conditions) and the reduced activation temperature is taken from  $E_a/R = 9800$  K as suggested in Chapter 3. Thermal conductivities and diffusion coefficients are calculated with the TRANFIT program in the CHEMKIN II code package [6.5] (polynomial regression versus temperature). Comparison between these calculated values and the values given in References [6.6], leads to the following results (Table 6.3.2.3-1).

**Table 6.3.2.3-1 Verification of mixture characteristics**

[H <sub>2</sub> ] dry conditions	$\sigma^*$	$\beta^*$	Le*	$\beta(\text{Le}-1)^*$	$\sigma$	$\beta$	Le	$\beta(\text{Le}-1)$
9 vol %	3.31	6.86	0.344	-4.5	3.26	6.77	0.377	-4.2
10 vol %	3.54	6.56	0.352	-4.3	3.48	6.48	0.383	-4.0
11 vol %	3.77	6.28	0.360	-4.0	3.71	6.21	0.389	-3.8
15 vol %	4.63	5.35	0.394	-3.2	4.55	5.29	0.411	-3.1

\* according to [6.6]

The values have some differences between 3% and 7% for  $\beta(\text{Le}-1)$  and lower than 2% for  $\sigma$  but not so important, and this could be included in the uncertainties.

### 6.3.3 Illustration

#### 6.3.3.1 Geometrical considerations

The chosen geometry corresponds to a French 900 MWe pressurized reactor with a large dry containment. The total volume is about 50 000 m<sup>3</sup> and the lumped-parameter nodalization uses 85 different compartments to describe the whole free volume.

With these "complex" definitions, the characteristic size of each compartment is given in Figure 6.3.3.1-1. In this calculation 85 nodes are considered with a free volume varying between 100 m<sup>3</sup> and 15 000 m<sup>3</sup> (upper dome region).

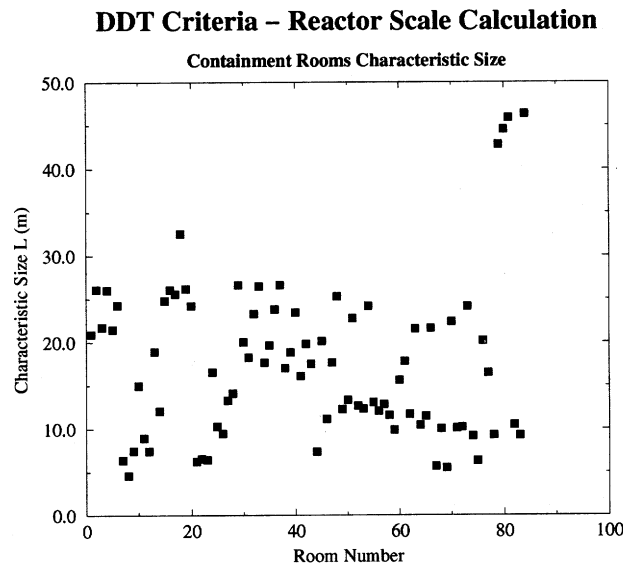


**Figure 6.3.3.1-1 Containment characteristic length L**

These calculated characteristic lengths vary from 5 m (small confined room in the lower part of the containment) and about 45 m (dome region) where all the "volumes" are open. This last length is quite the maximum length scale available in the containment (bottom of the pool and top of the dome), and this length scale can be used to validate the aggregation rules defined in Appendix F.

### 6.3.3.2 *Severe accident scenario*

In all the possible scenarios regarding PSA, it was decided to select two situations. The choice we made implies a scenario and also a selected time during the whole scenario. One can notice that the criteria could be directly implemented in the lumped-parameter code, and thus it will be useful to follow the value of the criteria during the whole scenario. In this current application, a post-processing methodology was chosen, and the criteria will only be evaluated at selected times during the scenario. The selected situations are as follows:

- Case 1: high hydrogen concentration (vol %) and low steam concentration. This corresponds to a small break (2-inch diameter) in the cold leg with failure of both the safety injection (SI) and the spray system. The selected time corresponds to just before the failure of the vessel's lower head. This scenario has slow in-vessel kinetics, and this means a large hydrogen production (more than 100% of the active part of the cladding), the release rate is also slow.
- Case 2: the preceding scenario is an unmitigated severe accident scenario, and now the same scenario as that used in case 1 is used but hydrogen mitigation countermeasures (catalytic recombiners) have been implemented in the calculation. The equivalent of 28 FR90-1500 (Siemens type) recombiners has been distributed in the containment geometry. The selected time is the time of maximum hydrogen concentration.

These 2 test cases have been calculated with the RALOC mod 4.0 Cycl AF lumped-parameter code. To illustrate the calculation, Figure 6.3.3.2-1 presents the total mass of hydrogen in the containment until the vessel's lower head failure, and Figure 6.3.3.2-2 compares the hydrogen and steam distribution in each control volume at the selected time.

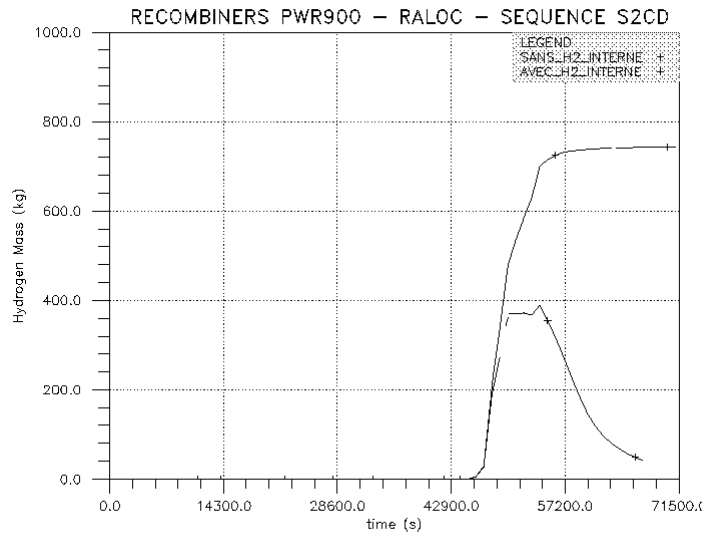


Figure 6.3.3.2-1 Severe accident scenario – hydrogen released mass

### Severe Accident Scenario – Lumped Parameter Approach

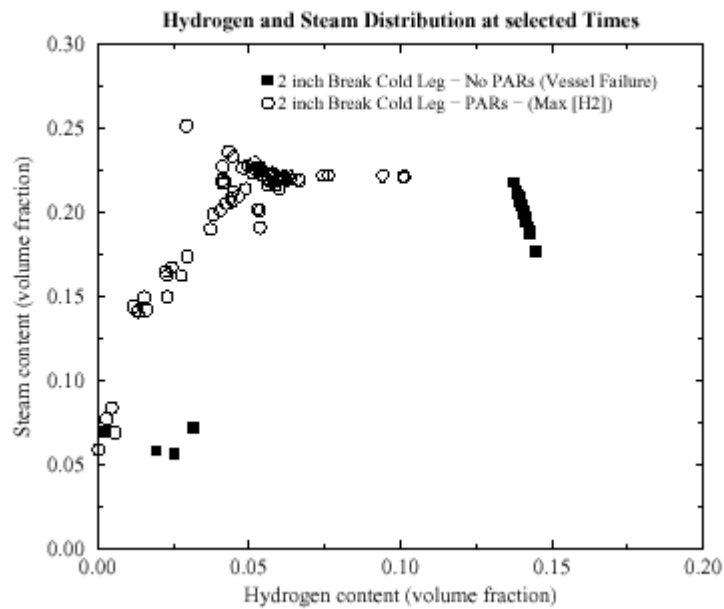


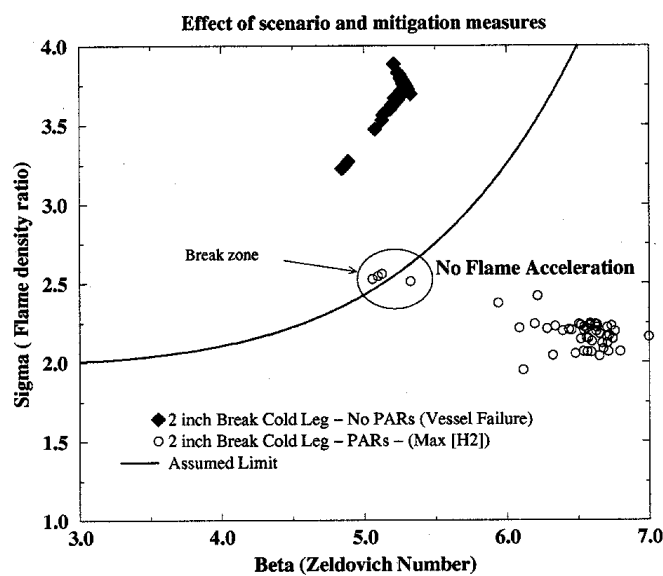
Figure 6.3.3.2-2 Severe accident scenario – hydrogen and steam distribution

These two test cases must be considered as an illustration of initial conditions for criteria application and not as results for all the possible scenarios involved in a level 2 PSA. Higher hydrogen release rates are expected during in-vessel core reflooding, for example.

### 6.3.3.3 Applications

#### 6.3.3.3.1 The $\sigma$ criterion

#### Flame Acceleration Criteria – Reactor Scale Calculation



#### Flame Acceleration Criteria – Reactor Scale Calculation

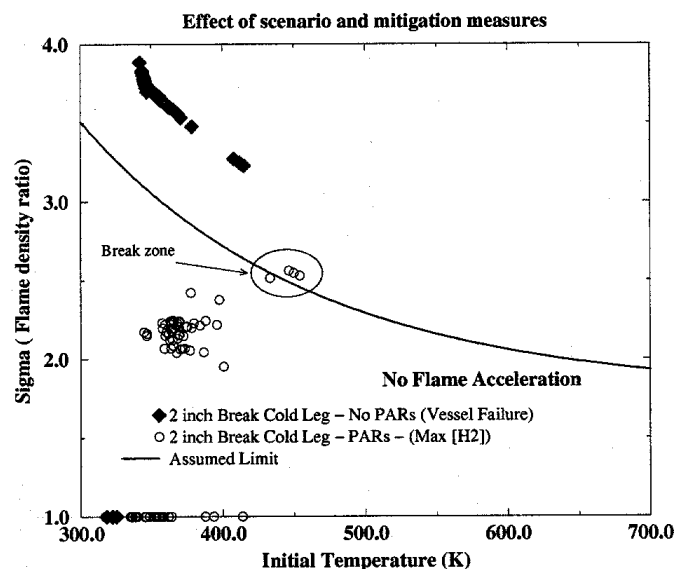


**Figure 6.3.3.3.1-1  $\sigma$  criterion application**

The  $\sigma$ -criterion has been expressed relating to Zel'dovich number  $\beta$  and initial temperature  $T_u$ , the results are the same. For the first scenario, most of the containment rooms are above the assumed

limit; thus, this scenario cannot be excluded according to FA potential (Figure 6.3.3.3.1-1). In the second one, (use of passive autocatalytic recombiners, PARs), because of hydrogen risk countermeasures most of the rooms that are below the limit except three or four rooms located near the break (in the break plume) and are close to the assumed limit. This situation has a very short time period regarding the whole scenario, and one can conclude that this scenario has a small probabilistic contribution to FA risk.

6.3.3.3.2. *The L/λ criterion*

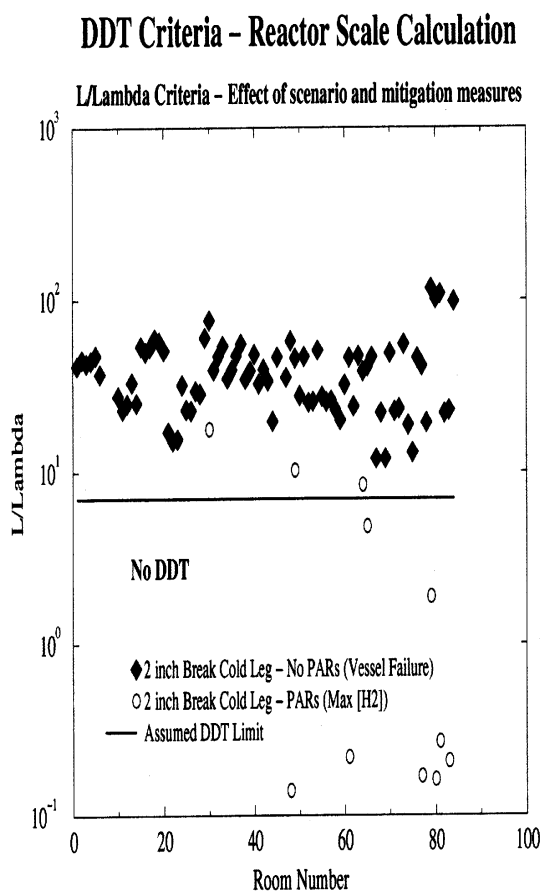


**Figure 6.3.3.3.2-1 L/λ criterion application**

For the first scenario, all the volumes are above the assumed limit (except non-flammable regions). This scenario is very sensitive to DDT because it was already sensitive to FA. Regarding fast transient phenomena associated to combustion process, this scenario represents one of the worst cases.

In the second scenario, the criterion is fulfilled in 3 rooms near the break (the neglected points have detonation cell sizes greater than 2 m because of very low equivalent ratio). For these 3 rooms, the criterion is perhaps not directly applicable because of too large hydrogen gradients (Figure 6.3.3.3.2-1). Nevertheless, this scenario is less sensitive to DDT as it also was for FA. According to a certain

level of flame acceleration needed for DDT occurrence, one can conclude that in this scenario, DDT is not expected to occur.

#### 6.3.3.4 *Uncertainties and conclusions*

Regarding uncertainties, many potential sources are listed in Chapter 3. The largest uncertainty seems to be on the detonation cell size value, but in the present study a decrease by a factor of 1.5 or 2 of the detonation cell sizes does not change the conclusions. For some scenarios, the mixture and the geometrical characteristics are far from the assumed limits, so the conclusions are clear and they can or cannot be excluded in terms of FA and DDT risk analyses. Regarding applications, characteristic length  $L$  is very difficult to estimate especially with large openings. For the scenario where the representative points are closer to the limits, one has to look carefully at uncertainties and also at time duration. The preceding criteria are necessary conditions; thus in a conservative approach the first step could be a strict application of the proposed criteria before a more detailed analysis is performed. Results of FA criterion can be used to make this deeper analysis on DDT criterion, for example.

The preceding applications are just an illustration of how to apply the proposed criteria in a lumped-parameter approach. General conclusions cannot be extrapolated without a systematic and probabilistic analysis of the possible scenario for a given type of NPP. Expert judgment is mainly needed to build the characteristic length  $L$  and to carefully look at the results, but, in a first step, fast running tools can be built to select the most sensitive scenarios before starting a more detailed analysis on combustion behaviour. Such tools can be used to implement the proposed criteria in a PSA approach.

## 6.4 Application of FA and DDT Criteria in CFD Codes\*

In the analysis of hydrogen behaviour in severe accidents, a chain of interconnected physical processes has to be modelled in a systematic way to arrive at mechanistic and unambiguous results for containment loads. Flame acceleration and DDT processes in a severe accident represent just two possible phenomena out of a large event tree. To clearly define the possible applications and limitations of the criteria described in Chapter 3 ( $\sigma$ - and  $\lambda$ -criteria) it is necessary to first describe the general structure of a complete self-consistent hydrogen analysis.

### 6.4.1 Methodology for Hydrogen Analysis

The modelling of hydrogen behaviour in severe accidents with CFD (and LP) codes requires information for a series of interconnected steps (Figure 6.4.1-1).

#### 6.4.1.1 Plant design

The starting point of any analysis is, of course, selection of the plant. This apparently trivial point is included explicitly into the general analysis procedure because the plant design has many important implications for later stages of the CFD analysis. For instance, the core size and type of reactor (PWR or BWR) will determine the maximum possible hydrogen source term, the free containment volume will influence hydrogen concentrations, and the distribution of steel and concrete masses, as well as surfaces, will affect the equally important steam concentrations.

The geometrical containment design, moreover, defines the mathematical boundary conditions for the solution of the 3D fluid-flow equations of the CFD model. The generation of a computational 3D grid for a complex reactor containment is a very demanding task, in terms of best-possible geometry representation and judgment about the effects of always necessary geometry simplifications. In fact, the experience in Germany with CFD modelling of three different plant designs has shown that a large part of the total analysis work is concerned with the 3D grid generation and corresponding quality control.

#### 6.4.1.2 Hydrogen mitigation system

For a given plant, the next important question for the hydrogen analysis concerns the mitigation system under consideration. For the components of this mitigation system, verified CFD models must exist to predict their efficiency and effects on hydrogen-relevant parameters in the further progression of the accident. The GASFLOW code has, for example, models for spark igniters, and many Siemens as well as NIS recombiners, which were validated on different test series, many of them performed in the Battelle Model Containment (BMC) [6.7,6.8]. If, for example, spark igniters and catalytic recombiners are chosen for the hydrogen mitigation approach, the number and location of each of these modules must be defined within the grid resolution of the CFD containment model.

---

\* Contributed by Dr. W. Breitung

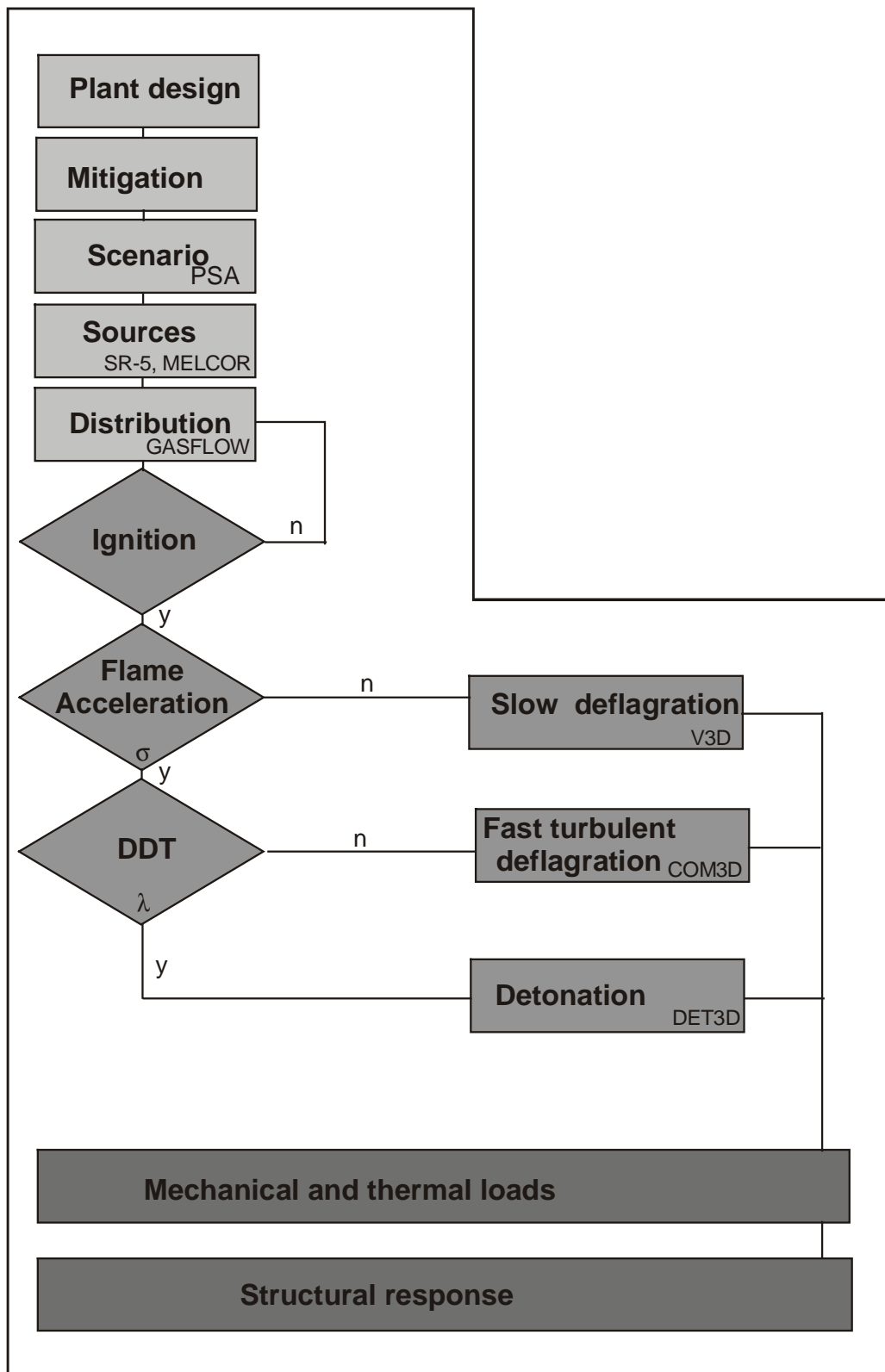


Figure 6.4.1-1 Outline of a complete self-consistent procedure for hydrogen analysis in severe accident research

### 6.4.1.3 *Accident scenario*

For a given plant and mitigation system, the next question is what type of severe accidents are physically possible within this installation, and which sequences should be covered in the analysis as representative cases.

Severe accidents require that all safety injection systems fail for an extended period of time (hours). All theoretically possible accident sequences can be grouped into relatively few accident categories, mainly different LOCAs and transients. It is not possible, nor necessary, to analyze all sequences with respect to their hydrogen risk.

In Germany, several criteria were formulated to select from the wide range of severe accidents a subset that covers the whole spectrum of possible requirements for hydrogen mitigation systems. In other words, looking from the perspective of system performance, the question is what are the most serious conditions mitigation systems that could be encountered in core-melt accidents, and which group of selected accidents produces these maximum requirements.

From this point of view, the selected hydrogen scenarios should include the major accident classes (LOCAs and transients), cover detrimental properties of the H<sub>2</sub>-steam source (large integral H<sub>2</sub> mass and release rate), and adverse containment conditions (e.g., low steam concentration at the beginning of H<sub>2</sub> release). Each accident will fulfil some of these criteria. Based on these and other considerations, five representative hydrogen scenarios were proposed for PWRs in Germany [6.9]:

1. surge-line LOCA;
2. small-break LOCA, 50 cm<sup>2</sup>, without secondary cooldown (heat sink) and including reactor pressure vessel (RPV) failure;
3. station blackout with depressurization of primary circuit and flooding of the core after recovery of the electric grid (no RPV failure).
4. loss of feedwater with primary-system depressurization and
5. steam generator tube rupture with open secondary circuit (bypass scenario).

These five selected hydrogen scenarios generate together a wide spectrum of conceivable adverse conditions for hydrogen control. Most other accident scenarios should be covered by these cases with respect to the hydrogen risk because they are not expected to generate new situations that are more difficult to control. On the other hand, the restriction of the analysis to only one or two hydrogen scenarios will leave questions open about the efficiency of the investigated mitigation approach for severe accidents in general.

#### 6.4.1.4 *Hydrogen and steam sources*

After definition of the relevant hydrogen scenarios, the next question is what hydrogen and steam-water sources must be expected for these cases. For fully consistent CFD calculations, the mass, momentum, and energy of these species are needed for the whole duration of the accident simulation. In addition, the location of the release must be specified.

In many cases, it will only be possible to derive complete H<sub>2</sub>-steam sources by combining parametric code calculations with best estimates for still uncertain hydrogen production processes.

In general, the H<sub>2</sub> and steam mass sources are best predicted for the early in-vessel phase although different code calculations for the same scenario still can vary significantly in the predicted timing of the gas generation. The uncertainties further increase with accident progression because the initial and boundary conditions for the metal oxidation reactions (temperatures, surfaces) as well as the physical phenomena become more and more unknown.

Only parametric models currently exist for the late in-vessel phase, which is dominated by debris and pool behaviour. For prediction of H<sub>2</sub> generation, the time-dependent temperature, Zr, steam, and interface distributions are required.

No applicable predictive models are currently available for hydrogen and steam production from

- oxidation of U-Zr-O melts,
- reflood of an overheated dry core,
- failure of the RPV,
- ex-vessel steam-metal interactions (benign and energetic modes).

The only late process with reasonably verified models is the core-concrete interaction, which also can contribute significant amounts of CO.

Finally, it should not be overlooked that a good database for **steam** release is also important because the fast combustion modes that have the highest potential for containment damage are sensitive not only to the hydrogen but also to the steam concentration.

#### 6.4.1.5 *Hydrogen distribution*

With known hydrogen and steam sources, the next task is to calculate their transport, distribution, and mixing with the air in the containment. The outcome from this step of the analysis should be temperature, pressure, and composition of the H<sub>2</sub>-air-steam atmosphere as function of time and location.

A large number of interconnected physical processes and thermo-physical properties must be modelled with high spatial resolution to obtain gas compositions within precision limits that allow meaningful simulations of hydrogen combustion processes. Reasonable research targets are prediction of hydrogen concentrations within a few absolute percent (e.g.,  $12 \pm 2\%$  H<sub>2</sub>), of steam concentrations within 5 absolute percent (e.g.,  $12 \pm 5\%$  H<sub>2</sub>) and spatial resolutions  $\leq 1 \text{ m}^3$  per computational cell. The most important modelling subjects are

- 3D compressible fluid flow,
- convective heat transfer between gas and structure,
- radiative heat transfer (with high steam concentrations and temperatures),
- condensation and vaporization of water,
- heat conduction within structures,
- turbulence modelling and,
- mitigation devices (recombiners, igniters).

One code that has been developed to treat the hydrogen distribution task with 3D CFD methods is GASFLOW [6.7,6.8]; another one is TONUS developed by CEA.

#### 6.4.1.6 *Ignition*

For typical severe accident sequences in large plants, flammable mixtures will be generally predicted by the distribution analysis for certain time and space regions. To start a combustion process and to generate any potential risk to the containment, an ignition event is necessary. At this stage of the analysis, time and location of the first ignition leading to stable flame propagation must be predicted.

Ignition sources can be classified into random and deliberate (igniters). When igniters are included in the analysis, location and time of the ignition event will be determined by the evolution and expansion of the H<sub>2</sub>-air-steam cloud in the containment. With correctly designed igniter systems, ignition will occur shortly after hydrogen release has begun in a region with low hydrogen concentration.

Without deliberate ignition, the location and time of the ignition event is not predictable in a deterministic way. A number of potential ignition sources can exist in a severe accident environment, as, for example, electric equipment, bursting pipes, and core-melt particles. In this case, the consequences of random ignition must be analyzed. An exception that allows a mechanistic calculation would be self-ignition of the hot H<sub>2</sub>-steam mixture near the break location.

In any case, an ignition must be either predicted mechanistically (self-ignition or igniters) or it must be postulated with respect to time and location. The inclusion of igniters can be viewed as a possibility to control the ignition event in such a way that it occurs under the apparently most favourable conditions, that is early in the accident before large hydrogen masses could accumulate in the containment. From the point of risk reduction, this approach to mitigate hydrogen by design seems better than an uncontrolled random ignition that may come too late.

The reliable prediction of the ignition event is important because it defines the end of the non-reactive phase of the accident and the beginning of the reactive phase, which can create the potential for containment damage.

#### 6.4.1.7 *Flame acceleration*

After ignition the flame starts initially as a slow quasi-laminar premixed H<sub>2</sub>-air-steam deflagration. It will preferentially propagate along the hydrogen concentration gradient towards the richer or dryer mixtures and into regions with high turbulence generation. This effect and also the self-induced turbulence from the expansion flow of the burned mixture behind the flame can induce a transition from slow laminar to fast turbulent deflagration.

The dominant influencing parameters for FA are the mixture composition, turbulence generation, confinement, and length scale. The  $\sigma$ -criterion, described in Chapter 3, can be used for conservative estimates of the FA potential. If the criterion is not fulfilled, a slow quasi-laminar deflagration must be expected, which should be modelled with an appropriate numerical tool (e.g., V3D at FZK). If the  $\sigma$ -criterion predicts FA, the question arises as to whether the mixture under consideration could also undergo a transition to detonation.

#### 6.4.1.8 *Deflagration to detonation transition*

For this branching point, the  $\lambda$ -criterion—described in Chapter 3—was developed to check for a certain minimum scale of the reactive cloud relative to its average detonation cell size. If the scale should be insufficient, a fast turbulent combustion must be modelled, for which, for example, the COM3D code was developed at FZK and the TONUS code at CEA. Otherwise, a detonation simulation is appropriate, e.g., with DET3D (FZK) or TONUS (CEA).

The three discussed transition criteria for

- ignition (inert to flammable),
- flame acceleration (slow to fast deflagration), and
- detonation onset (deflagration to detonation),

can be used to select the most probable combustion mode and the corresponding numerical models and codes. These criteria are useful and currently also necessary because the direct numerical simulation of the transition processes themselves is still in its infancy, mainly because of the much smaller length scales that need to be resolved. Mechanistic modelling of the ignition event requires, for example, resolution of the ignition kernel with detailed chemistry treatment; the flame acceleration process would require resolution of the laminar to turbulent transition; and for detonation onset, the resolution of the initial hot spots with strong ignition would be necessary.

It is important to note that the evaluation of the three transition criteria only requires information about the composition and geometrical size of the combustible mixture generated during a severe accident. This information is available from the preceding step of the analysis, namely the 3D distribution analysis. Therefore the 3 criteria can already be evaluated “on-line“ during the distribution calculation to check where and when different risk situations develop during the accident progression, namely

1. occurrence of flammable mixtures,
2. potential for flame acceleration to fast “sonic” flame speeds, and

3. possibility of detonation onset.

The criteria can hence give early indications of the maximum possible mechanical loads to the containment, without actually entering the reactive flow simulation. This offers an easy way to check and optimize the effectiveness of the mitigation measures introduced at the beginning of the analysis. If, for example, the exclusion of local detonations of a given size or energy content is a necessary requirement for the mitigation approach, the mitigation measures should be modified until the  $\lambda$ -criterion is fulfilled accordingly, including a reasonable safety factor to cover uncertainties from other steps in the analysis, e.g., hydrogen release rate or total mass.

In summary, the use of the described criteria offers two important functions for the analysis of hydrogen behaviour:

1. early estimates of the potential combustion regime and corresponding containment loads without the need for combustion calculations, and
2. branching from the distribution calculation into the appropriate tool for simulation of the detailed combustion process and the generated time and space-dependent containment loads.

#### 6.4.1.9 *Mechanical and thermal loads*

The further flow of the analysis is straightforward. The thermal and mechanical loads of the respective combustion process (slow deflagration, fast deflagration, or detonation) are evaluated from the 3D simulation by storing temperature and pressure histories at different containment locations. Which of these two load categories prevails is mainly determined by the time of first ignition. Early ignition leads to low-pressure amplitudes but high local thermal loads. Late ignition of an accumulated hydrogen-steam-air cloud can result in transient high-pressure loads but negligible temperature increase in the solid structures. In both cases, the same total combustion energy is released but on largely different time scales (hours versus seconds).

#### 6.4.1.10 *Structural response*

The calculated loads serve as input for the last step in the analysis, which is to determine the structural response. Thermal loads from standing diffusion flames should not lead to loss of containment integrity by failure of sensitive structural components, as, for example, electrical feedthroughs or seals of hatches. Moreover, equipment needed to terminate the accident should not be disabled directly by a high-temperature environment or indirectly by electric cable damage.

The mechanical loads from fast flames can include pressure waves, impulses, and possibly impacts from combustion-generated missiles. If fast combustion modes cannot be excluded with the chosen mitigation system, the outer containment shell represents the last barrier against radioactive release. A thorough investigation of the local dynamic structural response should then be undertaken to demonstrate containment integrity, which is the ultimate goal of the whole hydrogen analysis.

The investigation of the ultimate containment integrity under severe accident loads is complicated by the fact that a containment building consists of many different components with largely different mechanical and thermal responses. The spectrum ranges from thick concrete structures to elastic gasket in the equipment or personal hatches. Temperatures, pressure, and radiation loads in severe

accidents can also create complex synergy effects on the response of containment components, as was, for example, shown for elastic gasket materials [6.10].

## 6.4.2 Implementation of Transition Criteria

For a mechanistic 3D CFD analysis of hydrogen behaviour in severe accidents, it is very informative to implement the above-described transition criteria for ignition, flame acceleration, and detonation onset into the code used for simulation of the mixing and transport processes. This section gives a short description of the approach used in the GASFLOW code [6.7,6.8].

The ignition criterion will not be discussed further in detail because the present report concentrates on fast combustion regimes. Currently, the following very simple criteria are evaluated to determine

- a. flammability of the mixture:  $x_{H_2} > 5 \text{ vol } \%$  and  $x_{O_2} > 5 \text{ vol } \%$ ; and
- b. self-ignition:  $x_{H_2} > 5\%$ ,  $x_{O_2} > 5\%$ ,  $T > 800 \text{ K}$ .

Additional work is underway to more precisely quantify the effect of spark energy, length, and duration on the ignition event in  $H_2$ -air-steam mixtures of accident-relevant temperatures and pressures.

### 6.4.2.1 $\sigma$ -criterion

FZK has recently implemented the  $\sigma$ -criterion into the GASFLOW code to judge the possibility of a slow flame becoming turbulent and accelerating to high speeds. To include nitrogen-enriched mixtures that are generated by the burning process, a four-dimensional table of  $\sigma$ -values was calculated using the STANJAN-code [6.5], with the dependent variables of hydrogen, steam and oxygen volume fractions and temperatures. It is not necessary to vary the initial pressure because  $\sigma$  is independent of  $p_0$ . An example of this database is given in Figure 6.4.2.1-1 for  $H_2$ -air-steam mixtures at 373 K in the form of a  $\sigma$ -contour plot. The computations were performed using the STANJAN code [6.5]. The physically relevant  $\sigma$ -range is, of course, defined by the flammability limit. At 373 K the critical  $\sigma$ -value is  $2.9 \pm 0.1$  for lean mixtures and  $3.75 \pm 0.25$  for rich mixtures (light gray region). Flame acceleration is possible for larger  $\sigma$ -values (dark gray region).

For evaluation of the acceleration potential the following  $\sigma$ -index is defined in GASFLOW:

$$\sigma_{\text{index}} = \frac{\sigma(\bar{x}_{H_2}, \bar{x}_{H_2O}, \bar{x}_{O_2}, T)}{\sigma_{\text{critical}}(\bar{x}_{H_2}, \bar{x}_{O_2}, T)} \quad (6.1)$$

where the nominator is the expansion ratio of the average mixture in the specified compartment. The  $x_{H_2}$ ,  $x_{H_2O}$  and  $x_{O_2}$  are the average hydrogen, steam and oxygen concentrations in the specified compartment, respectively. The denominator is the critical expansion ratio of the average mixture. The idea in this approach is that when the  $\sigma$ -index is  $< 1$ , flame acceleration is excluded, whereas for  $\sigma_{\text{index}} > 1$ , there is potential for flame acceleration. [6.11]

The expansion ratio of the average mixture in Equation. (6.1) is evaluated by quadratic extrapolation from the computed  $\sigma$ -table. The critical expansion ratio is evaluated by interpolation from the data given in Chapter 3, which are listed in Table 6.4.2.1-1 as used in GASFLOW. Note that  $\sigma_{\text{critical}}$  is

independent of the steam concentration because the effect of dilutents (in all tests with He, Ar, N<sub>2</sub>, H<sub>2</sub>O, and CO<sub>2</sub>) could be condensed into one common value for  $\sigma_{\text{critical}}$ .

**Table 6.4.2.1-1 List of critical  $\sigma$ -values used in the GASFLOW model as function of temperature for lean and rich H<sub>2</sub>-air-steam mixtures.**

Temperature (K)	$\sigma_{\text{critical}}$	
	$x_{\text{H}_2} < 2 x_{\text{O}_2}$	$x_{\text{H}_2} > 2 x_{\text{O}_2}$
300	3.75	3.75
400	2.80	3.75
500	2.25	3.75
650	2.10	3.75

In summary the calculation of the  $\sigma$ -index includes the following steps in the CFD distribution calculation:

1. definition of the control volume, which should as much as possible agree with physical room boundaries; (The definition of a free largely unconfined control zone leads to unphysical and overly conservative results.)
2. calculation of the average mixture composition in this room; (Since the current database for derivation of the  $\sigma$ -criterion is almost exclusively based on homogeneous mixtures, transient time periods with strong mixture gradients in the considered compartment require additional investigations.)
3. calculation of the expansion ratio  $\bar{\sigma}$  for the average mixture using a  $\sigma(x_{\text{H}_2}, x_{\text{H}_2\text{O}}, x_{\text{O}_2}, T)$ -table to cover H<sub>2</sub>-air-steam-N<sub>2</sub> mixtures in general;
4. calculation of the critical expansion ratio  $\sigma_{\text{critical}}$  according to Table 6.4.2.1-1; and
5. evaluation of  $\sigma_{\text{index}} = \bar{\sigma} / \sigma_{\text{critical}}$ .

#### 6.4.2.2 The $\lambda$ -criterion

The described  $\lambda$ -criterion was implemented into the 3D field code GASFLOW as follows.

##### Step 1: Characteristic cloud dimension D

The characteristic dimension  $D_n(t)$  of the H<sub>2</sub>-air-steam cloud in room number n, which evolves from the source location is calculated from

$$D_n(t) = V_n(t)^{1/3} \quad (6.2)$$

$$V_n(t) = \sum_i \Delta V_{i,n}(t) \quad (6.3)$$

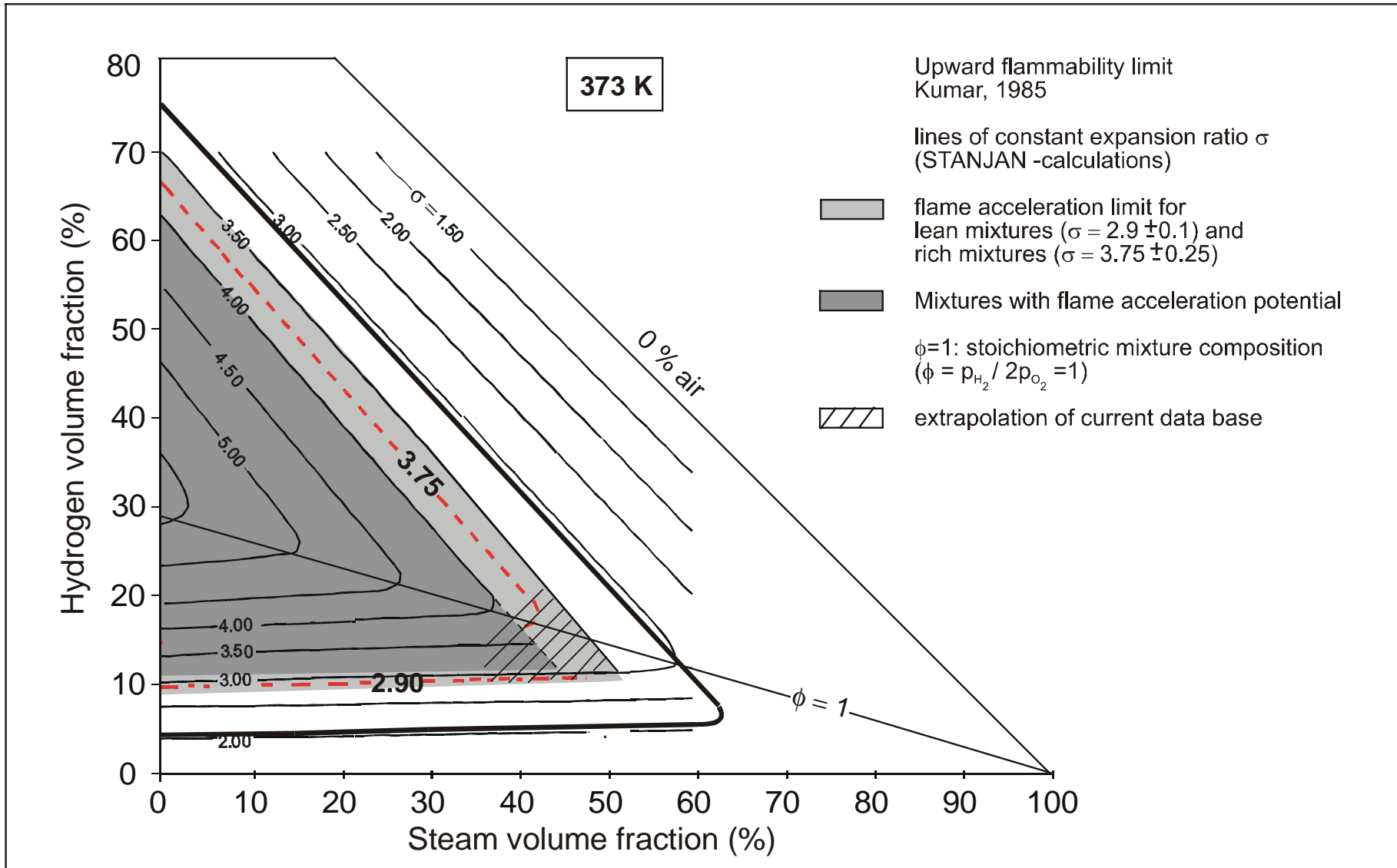


Figure 6.4.2.1-1 Expansion ratio and flame acceleration limits of hydrogen-air-steam mixtures at 373 K. [6.12]

where  $\Delta V_{i,n}$  are those computational cells in containment room  $n$ , which contain a burnable mixture at time  $t$ . In case of a dry  $H_2$ -air mixture, these are the grid cells containing between 4% and 75%  $H_2$ , the lower and upper flammability limits, respectively. To identify highly transient hydrogen release phases that can lead to enriched clouds embedded in a large cloud of low hydrogen concentration, the lower integration limit of 4%  $H_2$  can also be raised to 8% and 16% respectively.

### Step 2: Average detonation cell width $\lambda$

The average composition of the  $H_2$ -air-steam cloud in room  $n$  at time  $t$  is

$$[\bar{x}_{H_2}(t)]_n = (\sum x_{H_2,i} \cdot \Delta V_i)_n / V_n \quad (6.4)$$

$$[\bar{x}_{H_2O}(t)]_n = (\sum x_{H_2O,i} \cdot \Delta V_i)_n / V_n \quad (6.5)$$

where  $x_{H_2i}(t)$  = hydrogen volume fraction in cell  $i$  of the  $H_2$ -air-steam cloud in room  $n$ , and

$x_{H_2Oi}(t)$  = corresponding steam volume fraction.

This average composition is used to calculate the average equivalence ratio  $\phi_n$  of the cloud, which in case of  $H_2$ -air-steam mixtures is

$$\phi_n = 2.3866 \bar{x}_{H_2,n} / (1 - \bar{x}_{H_2,n} - \bar{x}_{H_2O,n}) \quad (6.6)$$

The average detonation cell width  $\lambda_n$  of the cloud mixture in room  $n$  can now be evaluated from measured or calculated data for  $\lambda_n(\phi, x_{H_2O})$ . The average composition and detonation cell size of the cloud is used here as measure for the detonation sensitivity because this evaluation method gave also good agreement with the  $7\lambda$ -correlation in the RUT tests with dynamic  $H_2$  injection into air.

### Step 3: DDT index $R$

At any given time during the calculation, a DDT index  $R$  is evaluated for room  $n$  according to

$$R_n(t) = \frac{D_n(t)}{7\lambda_n(t)} \quad (6.7)$$

If this ratio is less than 1, detonation transition is excluded or highly unlikely. If the ratio  $R_n$  is larger than 1, DDT cannot be excluded, according to the criterion.

### 6.4.3 *Examples for CFD Application*

The described methodology is first illustrated for a single-room geometry and then applied to a full-scale 3D multi-compartment reactor containment.

#### 6.4.3.1 *Singl- room geometry*

A single room of the BMC was chosen to show the principal use of the  $\lambda$ -criterion for a simple geometry. At the same time, this example is used to demonstrate the applicability of the  $\lambda$ -criterion for selection of a safe igniter position, which prevents a transition to detonation from an deliberate ignition [6.13].

Hydrogen is injected into the closed room of the BMC (Figure. 6.4.3.1-1). The room contains initially dry air at 1 bar pressure and 300 K. The vertical H<sub>2</sub> jet enters the room at the centre of the floor, the H<sub>2</sub> gas being at the same initial conditions (1 bar, 300 K, 21.6 g/s H<sub>2</sub>, velocity 1.0 m/s). Two cases will be discussed: a calculation with early ignition ( $R < 1$ ) and a calculation with late ignition ( $R > 1$ ).

##### 6.4.3.1.1 *Early ignition*

A GASFLOW analysis was performed with a glow plug igniter in the upper corner of the BMC room (Figure 6.4.3.1.1-1). This high location should cause an early ignition because buoyancy forces support the hydrogen transport into this direction.

The cloud dimension grows monotonically with time. At 12 s, the flammable edge of the H<sub>2</sub> air cloud reaches the igniter, which initiates a burn. The flame attaches to the source, reducing the cloud diameter of unburned gas to one or two computational cells. The hydrogen inventory in the room drops rapidly in response the burn. The DDT index  $R$  initially shows large values when only few cells above the release location are filled with a rich H<sub>2</sub> mixture.  $R$  then decreases quickly, and it is well below 1 at the time of ignition, so that no DDT potential could have existed. The fluctuations in  $R$  during the burn are due to the relatively rich but small standing diffusion flame. This diffusion flame does not represent a DDT threat.

##### 6.4.3.1.2 *Late ignition*

The second calculation involved an igniter at the worst-possible location, namely at the lowest and farthest position form the source (Figure 6.4.3.1.2-1). Hydrogen reaches this point only after the room is completely filled by the H<sub>2</sub>-air cloud. At ignition time the cloud dimension  $D$  is equal to the third root of the room volume  $[(41 \text{ m}^3)^{1/3} = 3.44 \text{ m}]$ . The calculated DDT index is well above 1. Almost 800 g of hydrogen burns after ignition, about 3 times more than in the early ignition case.

The DDT criterion predicts that in this late ignition case the deflagration could well develop into a local detonation [ $R(t_{\text{ign}}) \approx 10$ ]. At the time of ignition, the hydrogen concentration at the ceiling had reached 40%, a highly sensitive H<sub>2</sub>-air mixture.

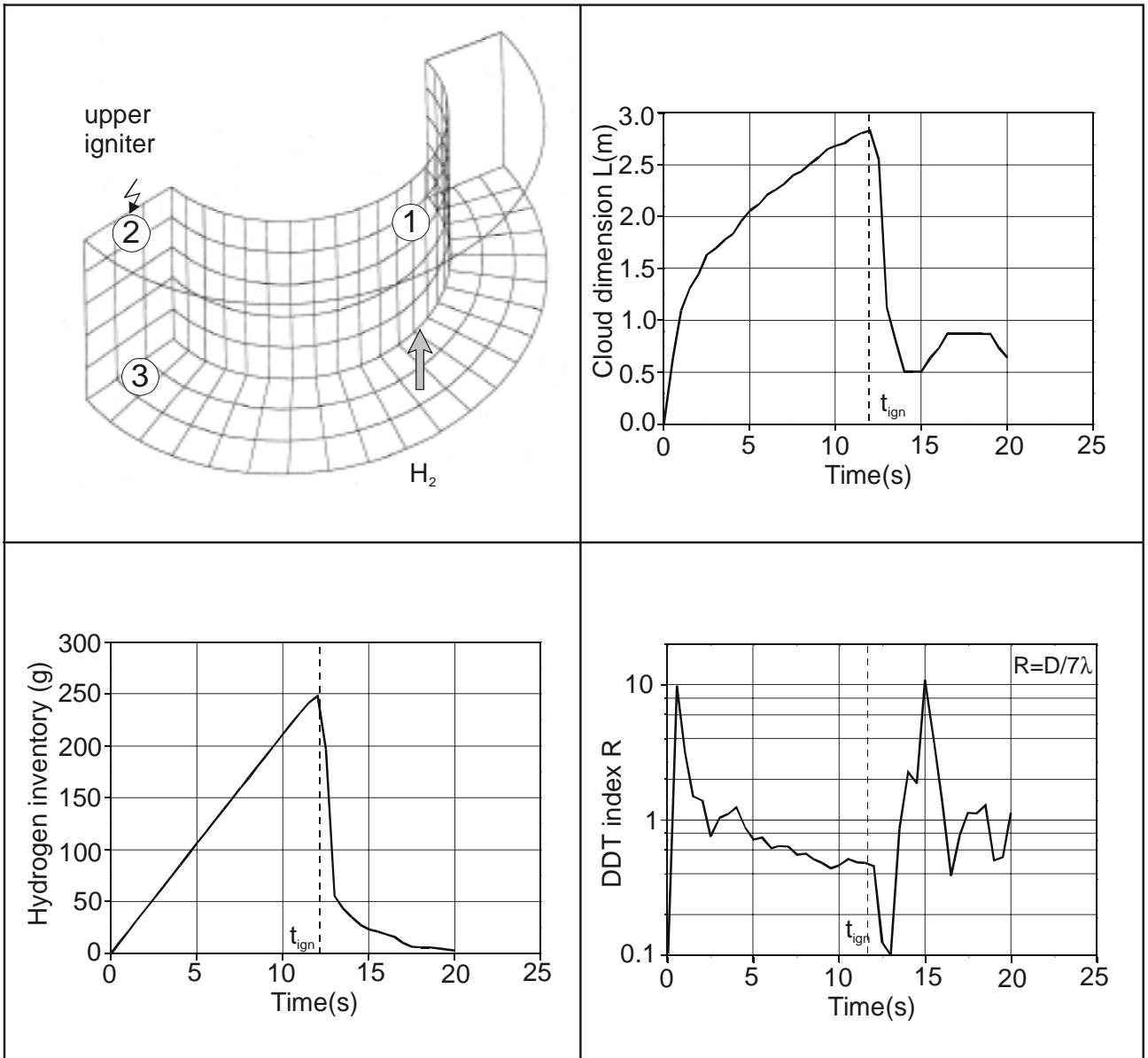


**Figure 6.4.3.1-1 Application of  $\lambda$ -criterion to single-room geometry, and results for H<sub>2</sub> injection with igniter in upper corner. Early ignition occurs with DDT index < 1.**

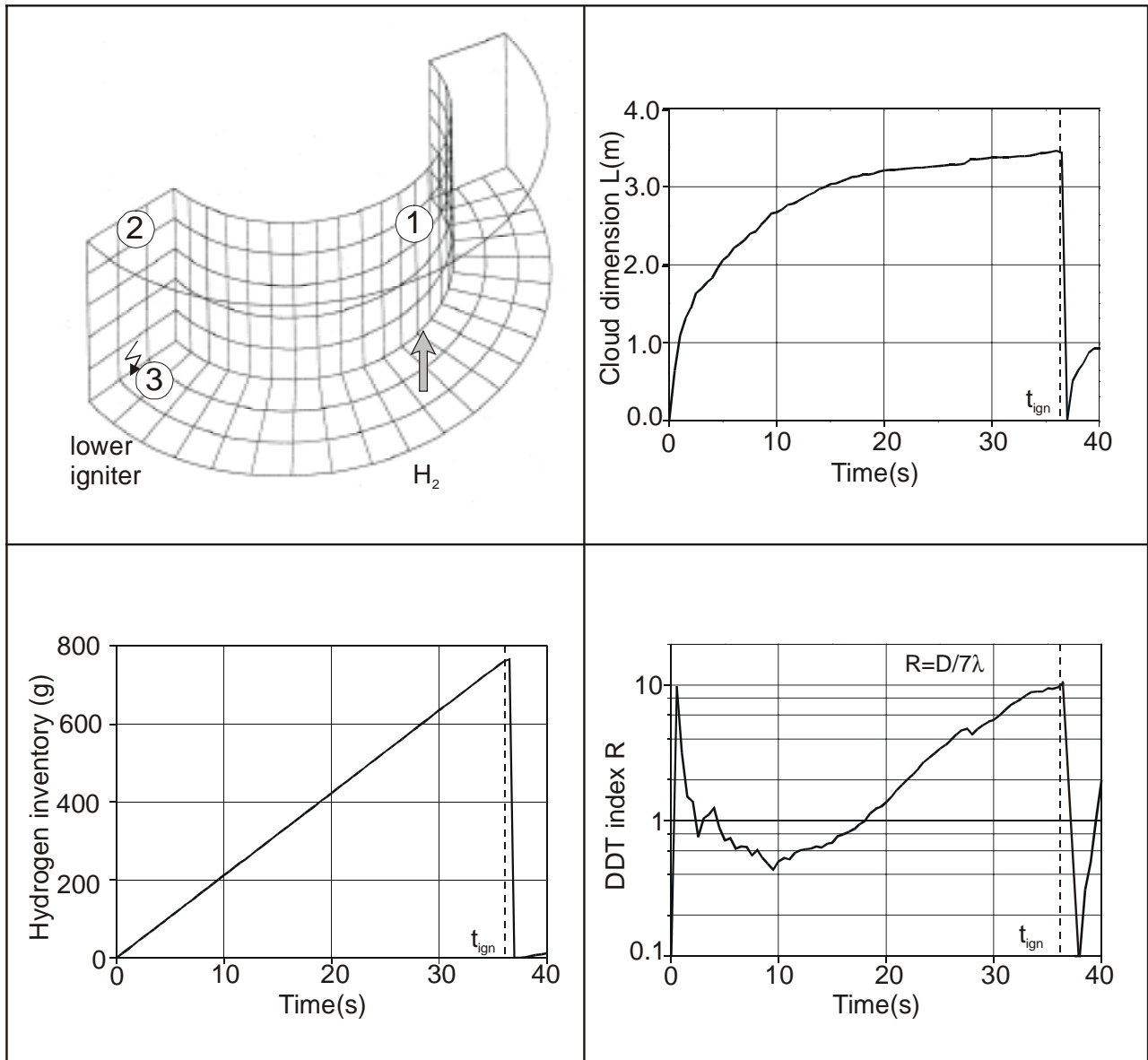


**Figure 6.4.3.1.2-1 Application of  $\lambda$ -criterion to single-room geometry and results for  $H_2$  injection with igniter in lower corner. Late ignition occurs with DDT index  $> 1$ .**

#### 6.4.3.2 Reactor containment

The example given in this section for a full-scale 3D reactor containment application follows the general methodology described in Section 6.4.1 and is summarized in Figure 6.4.3.2-1. The analysis includes the distribution simulation and the evaluation of the  $\sigma$ - and  $\lambda$ -criteria using the GASFLOW code. The calculations were part of a joint study between Siemens and FZK concerning hydrogen mitigation in an EPR design study [6.14].

**Plant design:** The investigated plant is a PWR with large dry containment, similar to the final design expected for EPR. The free gas volume is about 80 000 m<sup>3</sup>. The geometry model contain 139 000 computational cells. A glass model of the 3D containment structure is shown in Figure 6.4.3.2-1.

**Mitigation system:** For hydrogen mitigation a system of about 50 Siemens recombiners was located in the containment and accordingly modelled in the GASFLOW code. The recombiner model was verified against different test series in the Battelle Model Containment [6.15].

**Accident scenario:** The investigated accident sequence assumes an unprotected SBLOCA with late reflood of the overheated core. A high reflood rate is assumed so that the burst membrane ruptures, which normally closes the flow path from the primary system to the four internal refuelling water storage tanks' (IRWST) spargers). This event opens four release locations for hydrogen and steam (IRWST release in Figure 6.4.3.2-1), in addition to the break (break release in Figure 6.4.3.2-1).

**Hydrogen and steam sources:** The hydrogen and steam sources for this long-lasting scenario were calculated with MAAP, using very conservative modelling parameters for this particular study. The results are shown in Figure 6.4.3.2-2 for the time period during which hydrogen was released into the containment. The pre-conditioning phase with pure steam-water release prior to the onset of H<sub>2</sub> generation lasted about 24 500 s. The total hydrogen release amounts to about 700 kg H<sub>2</sub>, of which about 160 kg are released through the IRWST. The core reflood is estimated to produce about 400 kg of hydrogen.

**Hydrogen distribution:** The distribution of the described time-dependent steam and hydrogen sources in the containment were calculated with GASFLOW 2.1. Some results are shown in Figure 6.4.3.2-3 for the break room in which the hydrogen and steam source is located (see Figure 6.4.3.2-1). This room was modelled in GASFLOW by about 2500 computational cells, leading to an average volume per cell of approximately 0.4 m<sup>3</sup>. The average steam volume fraction in this room varies between 20% and 40%. The average temperature is about 400 K, whereas the maximum gas temperature reaches more than 1200 K in the immediate vicinity of the break. The average and maximum hydrogen concentrations reach their highest values during the reflood phase (Figure 6.4.3.2-3, top).

**Ignition:** No ignition by random sources such as, for example, electrical sparks was assumed.

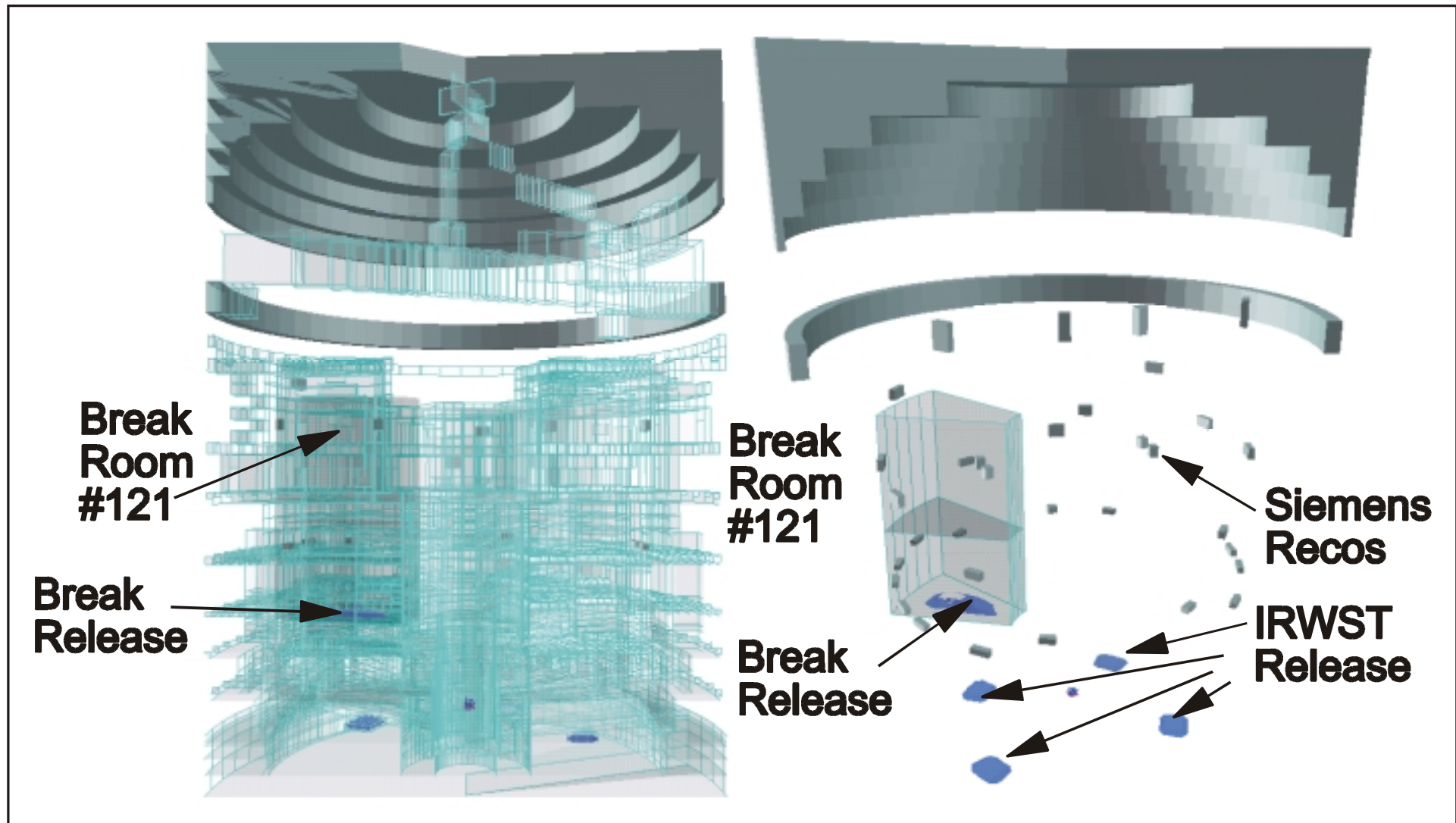


Figure 6.4.3.2-1 GASFLOW geometry model for the EPR design study (80 000 m<sup>3</sup> free gas volume, 139 000 computational cells)

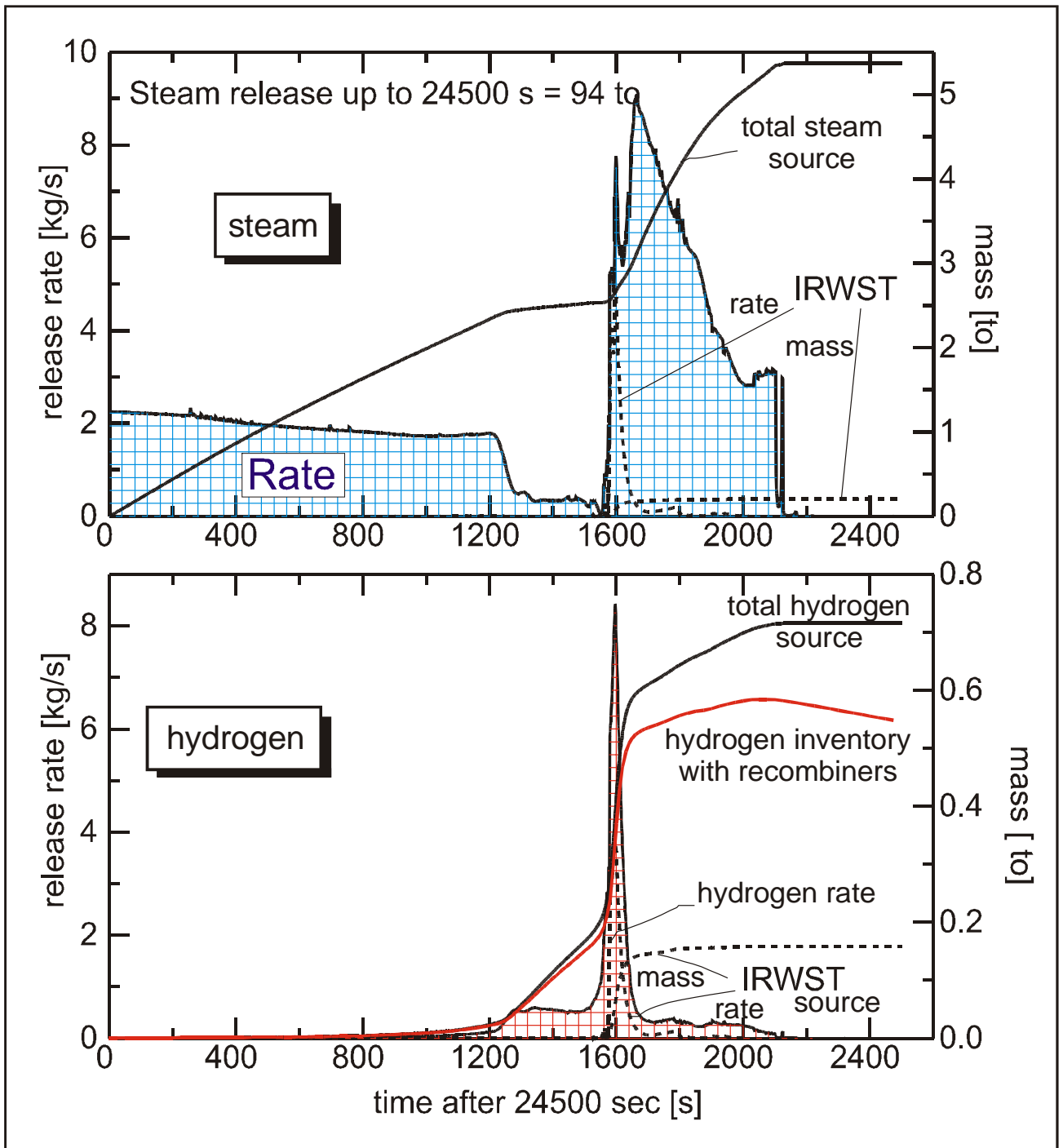
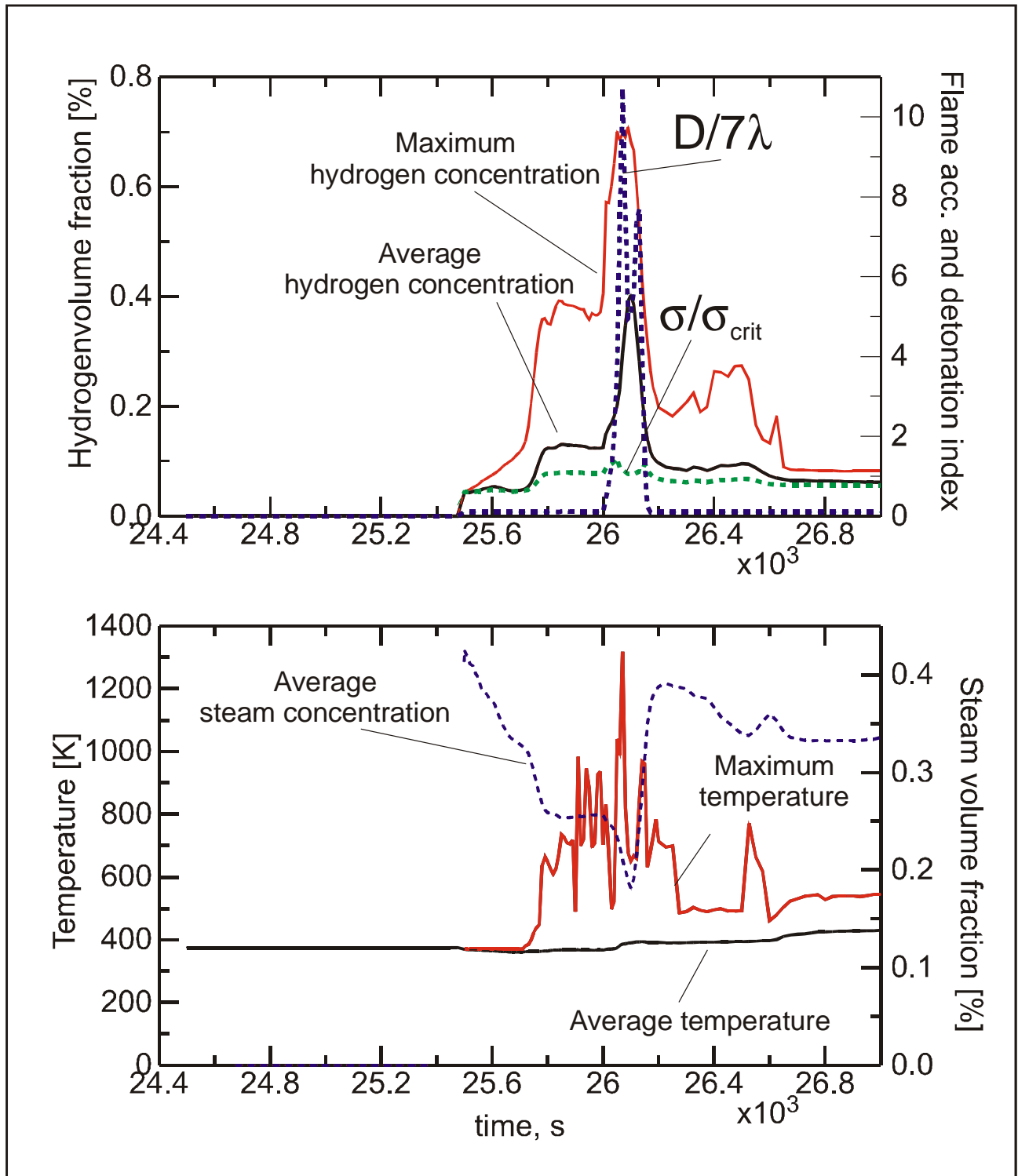


Figure 6.4.3.2-2 Steam and hydrogen sources used for a SBLOCA study of the EPR



**Figure 6.4.3.2-3 GASFLOW results for break room in SBLOCA calculations for EPR design study**

**Flame acceleration:** The flame acceleration index  $\sigma/\sigma_{\text{critical}}$  was evaluated for different rooms in the containment. The result for the break room is presented in the top graph of Figure 6.4.3.2-3. Values above one are reached shortly before and during the reflood event.

**Deflagration-to-detonation transition:** The corresponding result for the  $\lambda$ -criterion is also shown in Figure 6.4.3.2-3. DDT possibility exists only during the short reflood phase when, according to the

used MAAP result, a large H<sub>2</sub> release rate combines with a low steam release rate (Figure 6.4.3.2-1). During all other accident phases,  $D/7\lambda$  is much smaller than unity and DDT is excluded.

In summary, the FA and DDT criteria predicted that in the described scenario without ignition, using a quite conservative H<sub>2</sub>-steam release function, a potential for complete transition into detonation would only exist for short times during the reflood period.

#### **6.4.4 Example of Containment Section Analysis**

This section gives examples for full-scale reactor analysis using the tools described in the previous sections of this report. The first example concerns analysis of a combustion-related topic in a current German power plant, and the second example demonstrates the current abilities in simulating severe accident distribution and combustion processes for the design of a future severe-accident-resistant PWR.

The assessment of combustion loads on equipment (relief valves) to be installed in the annulus section outside the missile protection shield in the containment of BIBLIS-B (KWU design) has been subject to a simulation conducted by the help of the BASSIM code [6.16]. The outer wall of the annulus is the outer-containment steel shell. On the inner side, it is limited by the cylindrical missile protection shield. In a developed manner it has a length of 129.2 m, with a height of about 9.7 m. At intermediate height levels, there are partial subdivisions consisting of catwalks and walls. Larger openings to the dome section of the containment can be found in the area of staircases and four accumulators are placed there. Along the outer-containment steel shell, there is a gap all along the length of the annulus upwards and downwards. Inside the annulus, there are further installations and equipment, which may contribute to flame acceleration. A simplified top view of the annulus and the derived model representation is shown in Figure 6.4.4.-1. The potential locations of the relief valve casings were selected to monitor locations during the runs. A 2.5-dimensional representation of the annulus was chosen in order to save computational resources. This means the grid is two-dimensional with a variable thickness in the third dimension (here the annulus depth) for each cell. Thereby, a locally reduced flow channel width can be modelled. Recently, this approximated approach has been changed in the code to a full 3D representation. In the lower section of Figure 5.2.2.2-5 in Chapter 5 of this report, the developed model of the annulus is depicted. Apart from the pressure accumulators and the staircases, three different zones can be identified. In these zones, six porous regions are modelled to represent different degrees of blockage by obstacles, too small to be explicitly represented in the grid. To account for the increase of turbulence caused by porosity, additional terms are added to the  $k$ - $\epsilon$  turbulence model. The resulting grid with 130 x 32 cells is shown in Figure 6.4.4-2. From other experimental validation work it is known that the nodal resolution of the grid chosen is more a minimum to resolve the turbulence formation by obstacles and blockage. Specific investigations on grid convergence, however, have not been done so far. At the outflow areas from the computational domain, independent boundary conditions were set.

According to the German Risk Study, Phase B for a scenario with core-melt in the spatial area of the containment under discussion a hydrogen concentration of 8% combined with 25% of steam (80°C) was identified as what could be expected. The related system pressure was estimated to be 2.0 bar at the start of combustion. Finally, the existence of a hydrogen mitigation system was assumed and by this the presence of igniters in the annulus. Possible locations are indicated in Figure 6.4.4.-1.

The combustion model in the BASSIM code is the eddy dissipation model of Magnussen combined with the  $k$ - $\epsilon$  turbulence model. Prior to this study, the code underwent a number of validation steps with combustion experiments at different test facilities.

Examples of the flame progress through the annulus at different times can be seen in Figure 6.4.4-3. After about 16 s, the flame reaches the right end of the channel. Maximum gas speeds reached are in the range of 45 m/s. The pressure buildup until the end of the simulation is shown in Figure.6.4.4-4. It reaches about 0.5 bar overpressure, compared to the initial value. With 8% of hydrogen, its increase is restricted.

In summary, it can be concluded that, with ignition early taking place, FA and pressure differences over walls remain manageable, although a rather long channel with manifold obstacles is considered.

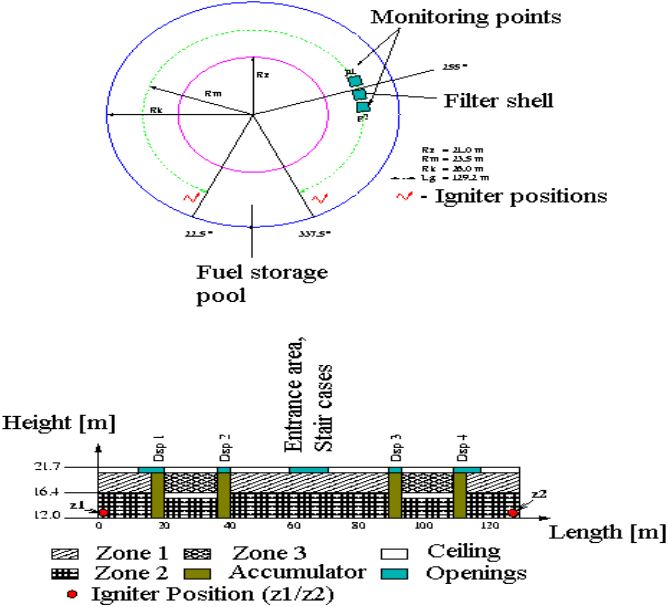


Figure 6.4.4-1 Annulus compartments and derived model

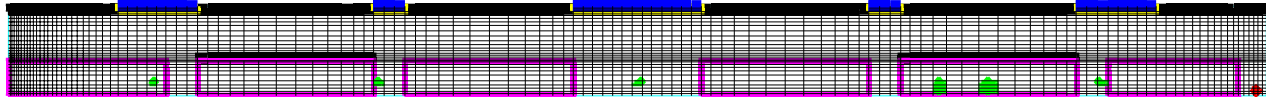
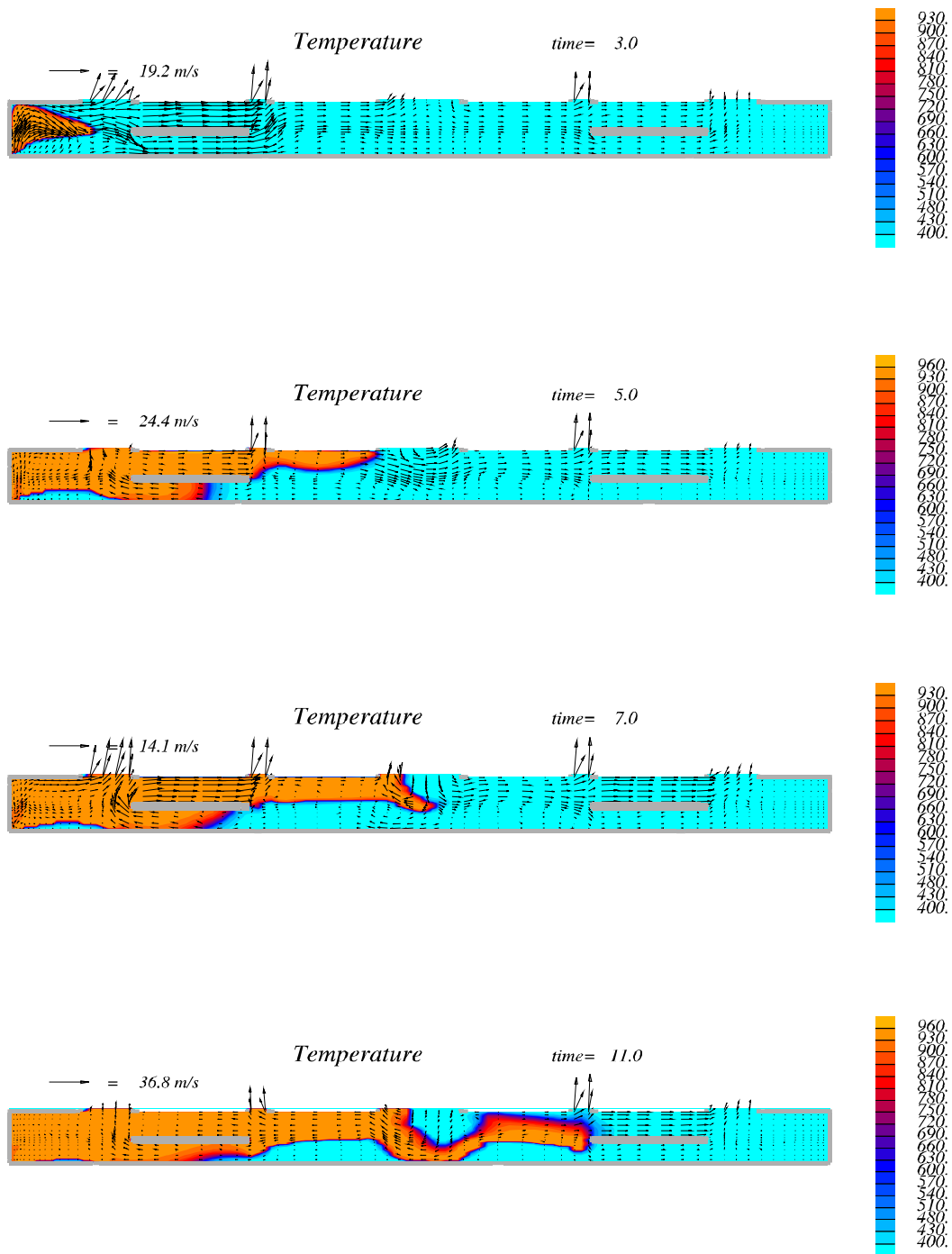
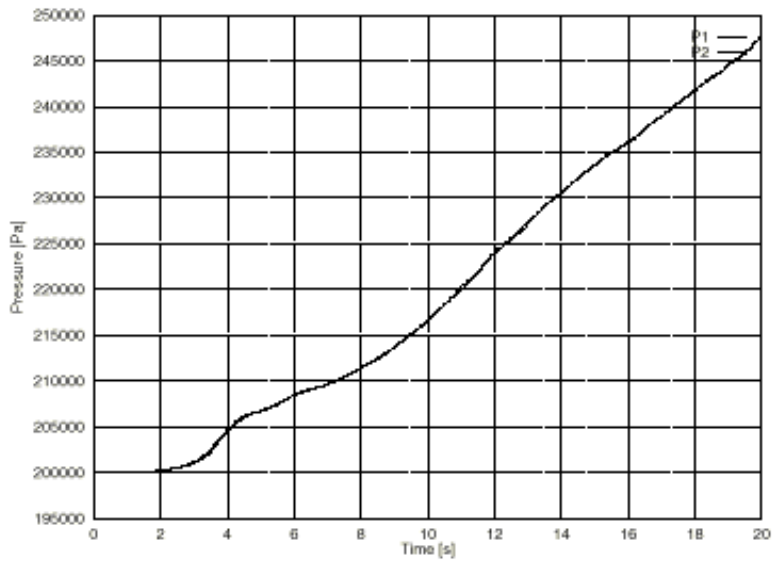


Figure 6.4.4-2 Computational grid



**Figure 6.4.4-3** Temperature contours in the annulus at different times of flame progress



**Figure 6.4.4-4 Pressure buildup during the simulation**

## 6.4.5 *Applications to Future Plant Analysis*

Section 6.4.5 summarizes the calculations of applications that have been done on hydrogen distribution, combustion, and loads for future plant design studies. The central goal of the future plant hydrogen work is to derive hydrogen control systems that fulfil the safety requirements for future LWRs, namely to show that the maximum amount of hydrogen that could be present during a severe accident can be confined without loss of containment integrity. In principle, there are two possibilities for hydrogen management in the future plants. The first one is to increase the strength of the containment design to the maximum possible combustion load. The second, more evolutionary way, is to use an existing containment design and install hydrogen control systems for load reduction, so that the original design load (LOCA) will not be exceeded.

### 6.4.5.1 *Base case*

First, a base case analysis without any hydrogen mitigation was performed for a LOOP scenario, to quantify the hydrogen situation in a future plant and to establish a baseline against which the need for and the effectiveness of hydrogen control measures can be compared.

In this dry LOOP scenario with only little steam injection from the IRWST water evaporation, a hydrogen stratification in the containment was predicted, ranging from about 9% to 13% H<sub>2</sub> (Figure 6.4.5.1-1). According to the criterion based on detonation cell size scaling ( $7\lambda$ -rule), a large detonation in the dome could not be excluded. The analysis was made for 90 000m<sup>3</sup> of free containment volume. This base case analysis with a detailed 3D containment model confirmed the development of hydrogen stratification in dry scenarios that were observed in earlier future plant calculations with a coarser computational grid (12 000 cells, [6.17]). The possibility of stratified containment atmospheres, together with the relatively large ratio of Zircaloy mass (core size) to free containment volume in the future plant design, makes additional hydrogen control measures mandatory.

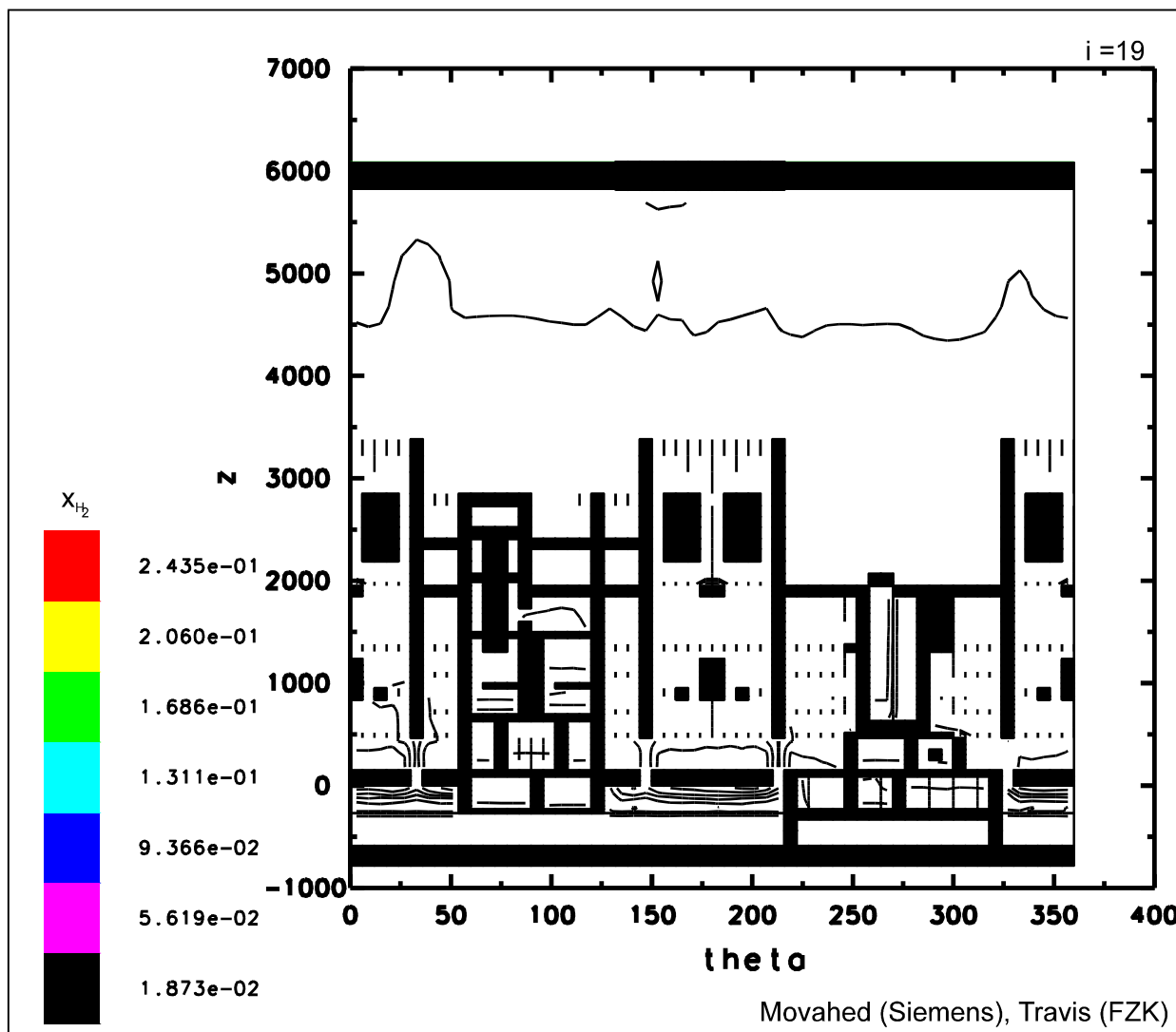


**Fig. 6.4.5.1-1 GASFLOW prediction for hydrogen distribution in LOOP scenario, MAAP sources, base case without hydrogen mitigation. The dry release leads to a stratified containment atmosphere ( $\approx 9\%$  to  $13\%$   $H_2$ ).**

#### 6.4.5.2 Mitigation with recombiners

##### 6.4.5.2.1 Distribution

The next step in the analysis of hydrogen behaviour was to include 44 catalytic recombiners of the Siemens design. Siemens selected the recombiner positions. The implementation in the GASFLOW model was done jointly by Siemens and FZK. The same hydrogen and steam source was used as before (LOOP scenario, MAAP sources).

The inclusion of this recombiner arrangement led to a decrease of the maximum  $H_2$  inventory in the containment from previously  $\approx 900$  kg to about 720 kg hydrogen. This relatively small decrease is due to the fact that the  $H_2$  release during the first heatup of the core is much faster (10 min) than the recombiner removal time (1 to 2 h). The relatively slow-acting recombiners, which remove typically several grams of  $H_2$  per second cannot significantly reduce the high initial release rate in the LOOP scenario (several kilograms per second). A rapid initial  $H_2$ -source occurs in practically all severe accident scenarios because the large chemical heat release of the Zr-steam reaction causes a fast self-accelerating temperature excursion during which initially large surfaces and masses of reaction partners are available.

The investigated 44 recombiners caused a substantial hydrogen reduction on the time scale of hours, but still allowed the accumulation of up to 720 kg of hydrogen in the containment. The next question therefore is what combustion mode and what structural loads after ignition would develop the resulting containment mixture.

#### 6.4.5.2.2 *Turbulent combustion*

The FA criterion, described in Chapter 3 and Section 5.4, predicts that the mixture present in the upper half of the containment (>11% H<sub>2</sub>), would be able to support FA. A COM3D calculation was therefore performed using the stratified H<sub>2</sub> distribution from the GASFLOW calculation as initial conditions (9% to 13% H<sub>2</sub>).

The future plant containment model of the COM3D code uses a cubic cartesian grid with 40-cm cell size, a total of 1.1 million computational cells, and about 80 000 m<sup>3</sup> free volume. The turbulent combustion is simulated with the verified extended eddy breakup model described in Section 4.3.3 of the report. The model performed well on different scales (FZK 12-m tube, RUT Facility) and for different H<sub>2</sub>-air- steam mixtures. The computation was made on the FZK-INR Cray J-90 using 4 of the 8 vector processors in parallel.

Figure 6.4.5.2.2-1 shows a plot of the H<sub>2</sub> concentration field 0.4 s after ignition on the right-hand side of the containment. The results are quite surprising and are non-trivial. The highest flame speeds (150 m/s) do not occur in regions of highest H<sub>2</sub> concentration, e.g., the dome, but rather in regions with both sufficient hydrogen concentration and turbulence generation, which is below the operating deck, and along the staircases. The highest loads to the outer containment wall (≤8.5 bar) develop on the containment side opposite to the ignition point because two propagating flame fronts meet here, leading to pressure wave superposition (top part of Figure 6.4.5.2.2-2). The right wall near the ignition point is loaded quite uniformly with pressures up to about 4 bar (bottom part of Figure 6.4.5.2.2-2). Because this pressure rise time is much longer than the typical containment wall period, this represents a quasi-static load to the structure.

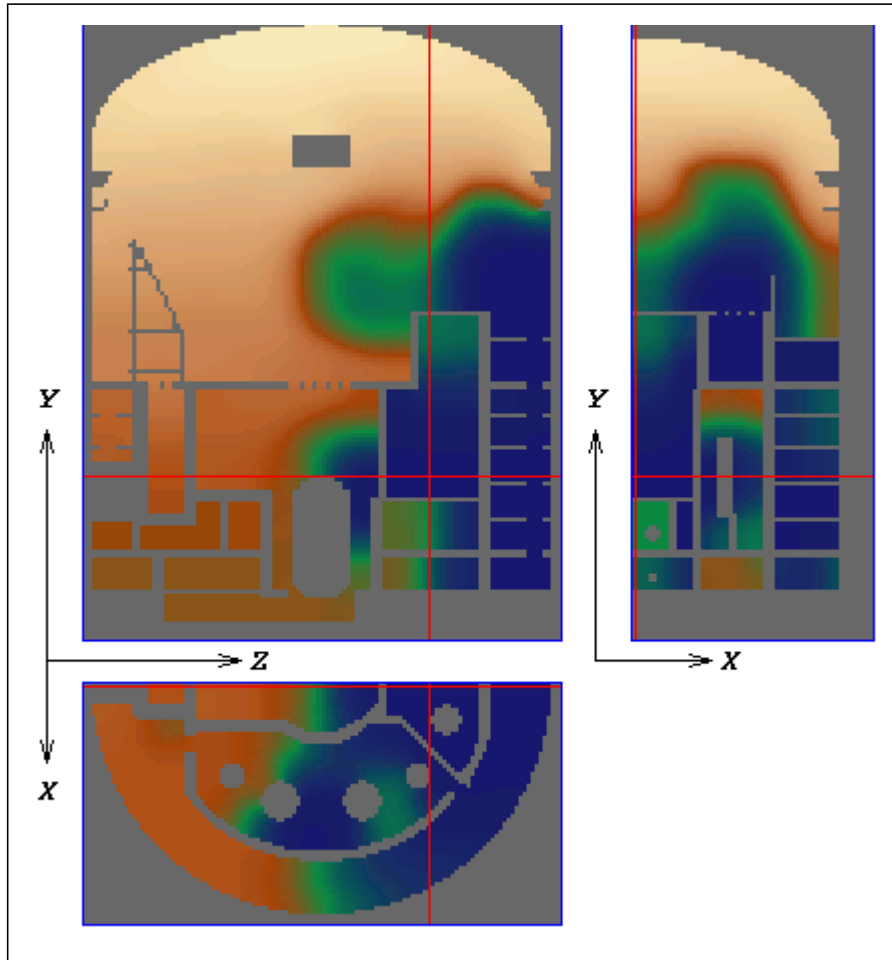
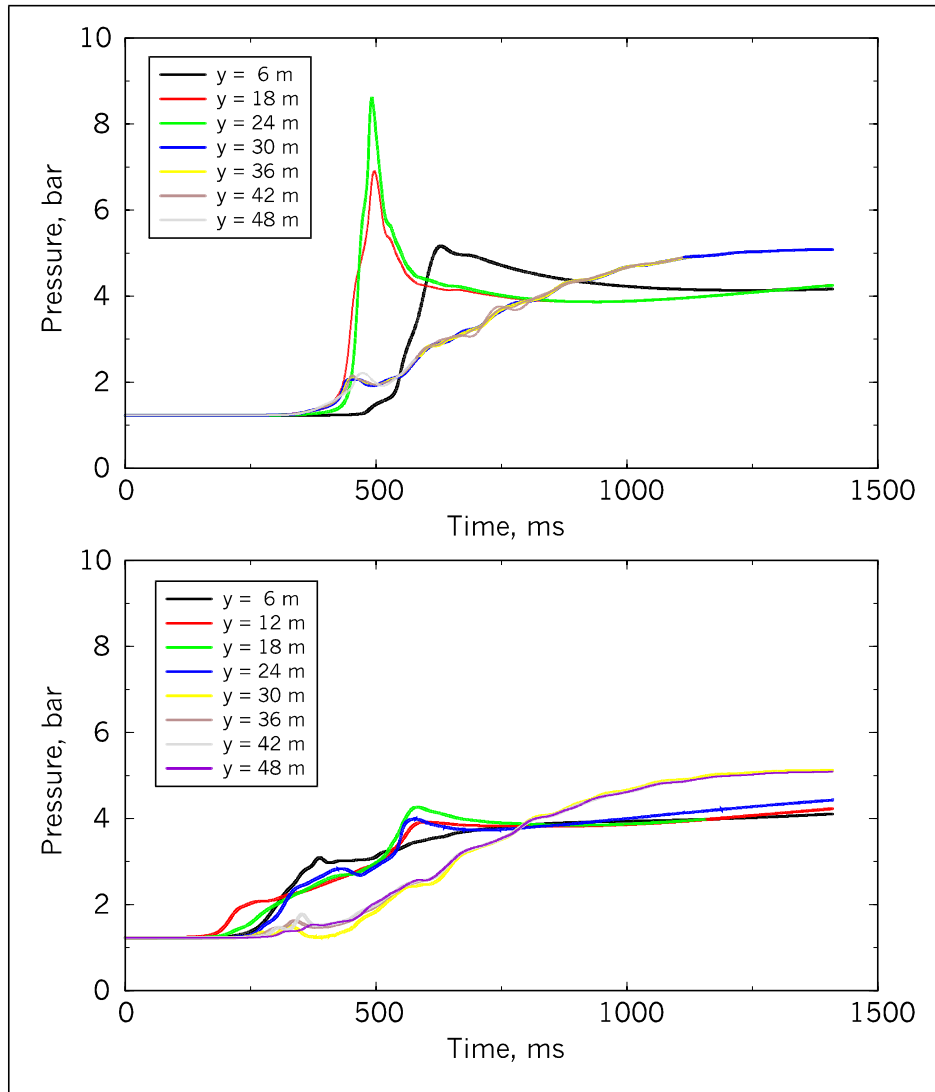


Figure 6.4.5.2.2-1 Simulation of turbulent combustion in the future plant with the COM3D code, 1.1 million computational cells, parallel computation on the FZK-INR Cray J90. The highest flame velocities (150 m/s) develop in regions where both sufficient hydrogen concentration and turbulence generation exist. Initial conditions from GASFLOW calculation, LOOP scenario, 44 recombiners.



**Figure 6.4.5.2.2-2 Containment loads from fast turbulent combustion in future plant, 3D COM3D calculation, initial gas distribution from GASFLOW, LOOP scenario, 44 recombiners installed. Top: pressure on the left containment wall, opposite from ignition point. Bottom: pressures on right containment wall near ignition point.**

The characteristic loading times of the left and right containment wall are quite different, about 50 ms and 300 ms, respectively. When compared to the typical natural response times  $T_{\text{cont}}$  of a dry PWR concrete containment [6.18], the first case represents a dynamic load, ( $T_{\text{load}}/T_{\text{cont}} \ll 1$ ), and the second case a load regime that is in the transition from dynamic to quasi-static ( $T_{\text{load}}/T_{\text{cont}} \approx 1$ ). In the first domain, the deformation is proportional to the wave impulse, whereas in the quasi-static domain it is proportional to the peak pressure reached.

#### 6.4.5.2.2 *Local detonation*

Application of the previously outlined DDT criterion to the calculated hydrogen distribution leads to the result that the mixture in the dome is sufficiently sensitive and large enough to support a detonation, provided a local FA would take place. The loads from such an event were estimated by a calculation using the detonation code DET3D, developed at FZK (Figure 6.4.5.2.3-1). The same computational grid as in the COM3D calculation was used. The origin of the detonation was assumed near the crane support on the left-hand side of the building where some turbulence-generating structures are located. This scenario should result in an upper limit for fast local combustion loads, which could be possible with the hydrogen inventory in the containment under the present conditions (LOOP, MAAP sources, GASFLOW distribution, 44 recombiners). A linear H<sub>2</sub> gradient from 7% to 13% was assumed, leading to a total H<sub>2</sub> mass of 690 kg in the containment. The initial temperature was 320 K, and the initial pressure 1.23 bar. Figure 6.4.5.2.3-2 shows the predicted pressure loads at different points along the upper edge of the containment cylinder (1 to 7). Ignition is initiated at point 1. In points 2, 3, and 4 basically side-on pressures are generated, whereas in points 5, 6, and 7 higher reflected pressures appear. Because of the short loading times of typically 10 ms, these loads clearly fall into the impulsive regime, where the building deformation is proportional to the wave impulse. The calculated impulses in the detonation wave range from about 5 to 20 kPa.

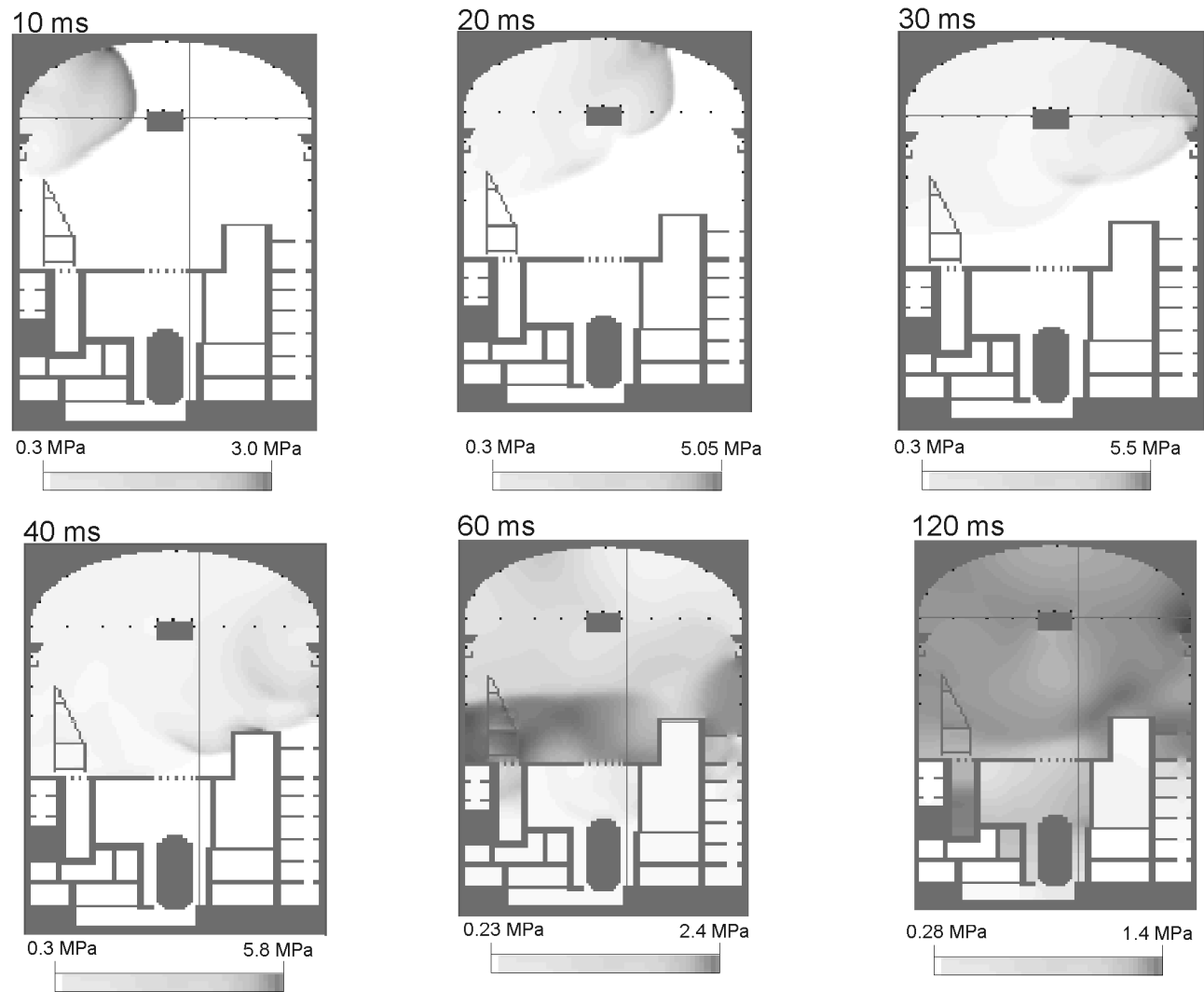


**Figure 6.4.5.2.3-1 Simulation of a local detonation in the containment dome**

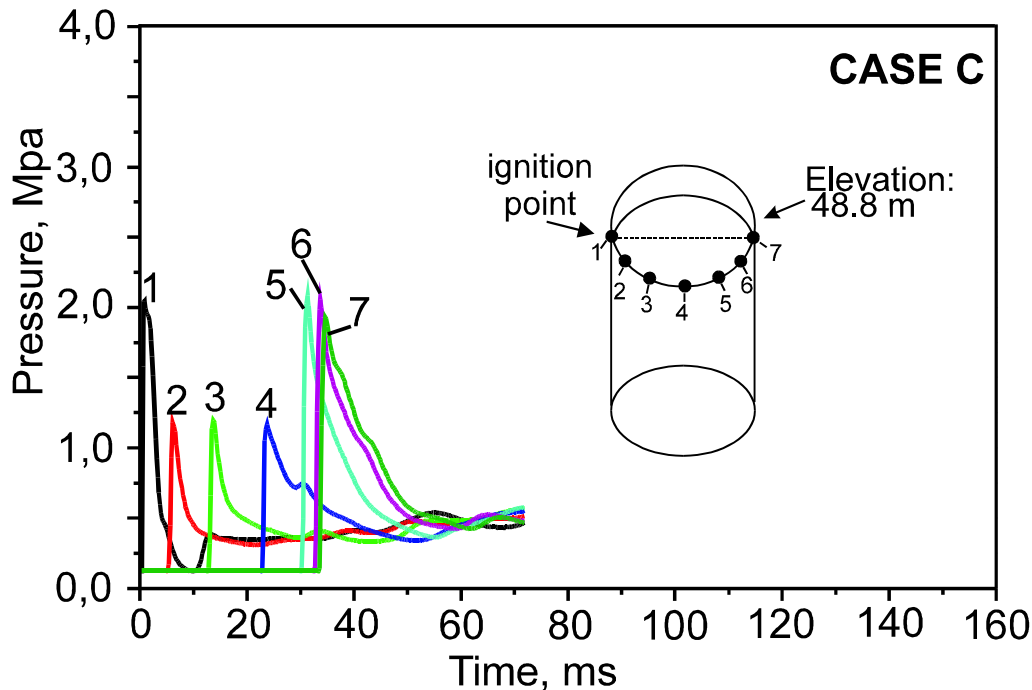


**Figure 6.4.5.2.3.-2** Calculated pressures from a local detonation in the containment dome. Total H<sub>2</sub> inventory in the building 690 kg H<sub>2</sub>, vertical H<sub>2</sub> gradient from 7% to 13% H<sub>2</sub>, initial pressure 1.23 bar, initial temperature 47°C, LOOP scenario with 44 recombiners .

#### 6.4.5.2.4 Results

The described calculations have shown that mitigation with recombiners alone still allows accumulation of up to roughly 700 kg H<sub>2</sub> in the containment and that combustion of this hydrogen mass could lead to significant dynamic loads. Although these loads may not endanger the containment integrity in the undisturbed areas, they would certainly require extensive analysis of containment integrity in regions around penetrations. Moreover, these dynamic loads could have severe consequences for safety systems that are needed for further management of an accident. Especially vulnerable are the structurally weak recombiner boxes and the spray system.

A general conclusion from these investigations is that early deliberate ignition in severe accidents, e.g., by igniters, appears necessary for further reduction of the maximum possible hydrogen inventory and of the corresponding pressure loads. Recombiner systems alone will not allow one to fulfil the new safety recommendations for future plants at least for dry LOOP scenarios. Therefore, an analysis with recombiners and igniters was performed.

#### 6.4.5.3 Mitigation with recombiners and igniters

In addition to the 44 recombiners, one igniter was installed at each of the four IRWST exits from which the hydrogen-steam mixture would emerge in dry scenarios. Again, the MAAP sources for the LOOP scenario with reflood were used as input to the GASFLOW code.

In the simulation, the first ignition occurred at a hydrogen inventory of 110 kg in the building. Thereafter a continuous burn was predicted, with one large standing flame at each IRWST exit (Figure 6.4.5.3-1). The evaluation of the  $7\lambda$ -criterion, as it is implemented in GASFLOW, showed that at no time was there a possibility of a DDT occurring and that a safe implementation of igniters is possible for the LOOP scenario. The early ignition, with most of the hydrogen still in the IRWST as a non-flammable mixture, reduced the maximum combustion pressure effectively to insignificant values.

The use of igniters basically transforms the previously large containment pressure load to a thermal load. The combustion energy is not released in a short event (seconds), but rather over a long time period (several thousand seconds). The thermal power of the diffusion flames can be quite high (1kg H<sub>2</sub>/s  $\equiv$  120 MW). Experimental investigations at the Russian Academy of Sciences on the stability limits of H<sub>2</sub>-air-steam diffusion flames, [6.19] have shown that the flame length will be in the range of 20 to 200 times the fuel gas exit diameter, depending on the Froude number and gas competitions. The flame length is governed by the exit velocity of the fuel gas (plume or jet).

Because of the potentially large thermal power and geometrical extension, the thermal effects of standing diffusion flames should be investigated in future work. The results can then be used to avoid thermal overloads to safety systems (igniters, recombiners, spray, liner) by design modifications, if necessary .

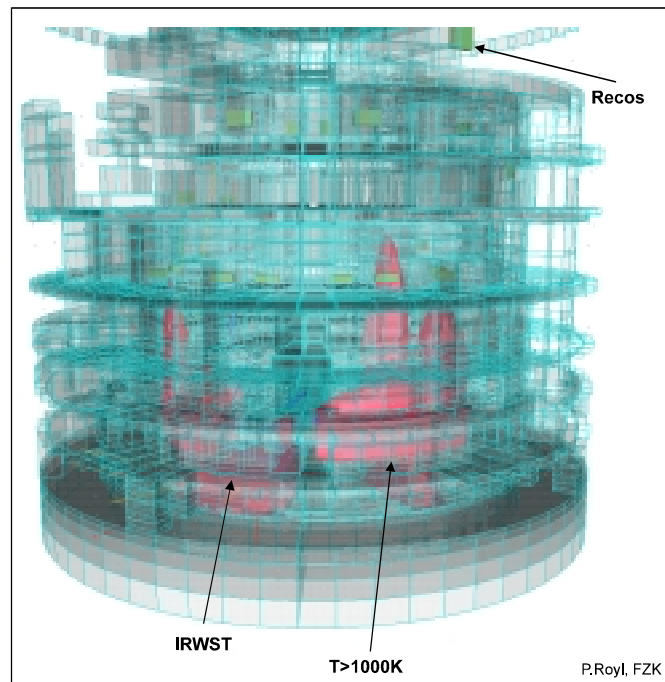


**Figure 6.4.5.3-1: GASFLOW analysis of LOOP sequences with 44 recombiners and 4 igniters at the IRWST exits. Low hydrogen inventories, low-pressure loads, and standing flames are predicted.**

#### 6.4.5.3 Conclusions

Theoretical tools for the analysis of distribution and combustion process in severe accidents were used to investigate the effectiveness of different options for future plant hydrogen mitigation systems. The problems analyzed in Sections 6.4.3.2 and 6.4.5 for example., lead to different outcomes. In the first case, only a short time window for fast deflagration was detected from the criteria. In the second case, a long-term combustion potential was predicted, and the analysis was conducted through the possible chain of combustion regimes up to detonation propagation. The goal of future reactor containment analyses is to fulfil new safety requirements for future reactors, which require control of the maximum amount of hydrogen that can accumulate in the containment building during a low-pressure scenario. Although a mitigation system consisting only of recombiners would be attractive for acceptance and cost reasons, the magnitude of the still-possible combustion loads makes the installation of additional deliberate ignition sources highly desirable. The calculations, done so far, have shown that igniters can be safely positioned and that they reduce the pressure loads very effectively. The described analysis tools allow us to exam relative merits of different mitigation schemes.

## 6.5 REFERENCES

- [6.1] S.B. Dorofeev, A.S. Kochucko, A.A. Efimenko and B.B. Chaivanov Evaluation of Hydrogen Explosion Hazard, Nuclear Engineering and Design, Vol. 148, 1994 305-316.
- [6.2] M.P. Sherman, S.R. Tieszen and W.H. Benedick, The Effect of Obstacles and Transvers Venting on Flame Acceleration and Transition to Detonation for Hydrogen-Air Mixtures at Large Scale, NUREG CR-5275, FLAME Facility.
- [6.3] R. Klein et al. (to be published) Contract FI4S-CT-96-0026, Models and Criteria for Prediction of DDT in Hydrogen/Air/Steam Systems under Severe Accident Conditions.
- [6.4] AE, W. Klein-Hessling, S. Arndt, M. Heitsch and B. Huttermann, GRS internal Report GRS-A-2308, RALOC mod4.0 cycl.
- [6.5] W.C. Reynolds, The Element Potential Method for Chemical Equilibrium Analysis : Implementation in the Interactive Program STANJAN, Dept of Mechanical Engineering Stanford Universtiy, Palo Alto, CA, 1986.
- [6.6] S. Dorofeev et al, Effect of Scale and Mixture Properties on Behaviour of Turbulent Flames in Obstructed Areas, .IAE-6127/3 or FZKA-6268, 1999.
- [6.7] J.R. Travis, P. Royl, R. Redlinger, G.A. Necker, J.W. Spore, K.L. Lam, T.L. Wilson, B.D. Nichols and C. Müller, "GASFLOW-II: A Three-Dimensional Finite-Volume Fluid-Dynamics Code for Calculating the Transport, Mixing, and Combustion of Flammable Gases and Aerosols in Geometrically Complex Domains, Vol.1, Theory and Computational Model, Reports FZKA-5994, LA-13357-MS, 1998.
- [6.8] J.R. Travis, P. Royl, R. Redlinger, G.A. Necker, J.W. Spore, K.L. Lam, T.L. Wilson, B.D. Nichols and C. Müller, "GASFLOW-II: A Three-Dimensional Finite-Volume Fluid-Dynamics Code for Calculating the Transport, Mixing, and Combustion of Flammable Gases and Aerosols in Geometrically Complex Domains, Vol. 2, User's Manual, Reports FZKA-5994, LA-13357-MS, 1998.
- [6.9] J. Rohde and W. Breitung, Selection of Representative Accident Sequences for Design and Evaluation of H<sub>2</sub>-control Measures in PWR-containments, 141<sup>st</sup> Session of RSK Light Water Reactor Committee, January 30, 1997.
- [6.10] P. Vanini, P. Becue, A. Orden Martinez, G. Forasassi and E. Pinno, Benchmark on Containment Penetration Sealing Areas Behaviour, FISA-97 Symposium on EU Research on Severe Accidents, Luxembourg, Nov. 17-19, 1997, 303.
- [6.11] W. Breitung and S.B. Dorofeev, Criteria for Deflagration-to-Detonation Transition (DDT) in Nuclear Containment Analysis, SMiRT-15 Post-Conference Seminar on Containment of Nuclear Reactors, Seoul, Korea, August 23-24, 1999.
- [6.12] R.K. Kumar, Flammability Limits of Hydrogen-Oxygen-Diluent Mixtures, Journal of Fire Sciences, Vol.3, 1985.
- [6.13] W. Breitung, S.B. Dorofeev and J.R. Travis, A Mechanistic Approach to Safe Ignitor

Implementation for Hydrogen Mitigation, Proc. of the OECD/NEA/CSNI Workshop on the Implementation of Hydrogen Mitigation Techniques, Winnipeg, Manitoba, May 13-15, 1996, AECL Report, AECL-11762; CSNI Report, NEA/CSNI/R(96)8; March 1997, 199-218.

- [6.14] M. Movahed, H. Petzold, J.R. Travis, P. Royl and G. Necker, private communication, July 1999.
- [6.15] P. Royl, W. Breitung, J.R. Travis, H. Wilkening and L. Seyffarth, "Simulation of Hydrogen Transport with Mitigation Using the 3D Field Code GASFLOW", 2<sup>nd</sup> Int. Conf. on Advanced Reactor Safety, Orlando, FL, USA, June 1-4, 1997.
- [6.16] K., Fischer, A. Kneer and A.K., Rastogi, Berechnung von, H<sub>2</sub>- Deflagrationslasten auf Entlastungsfiltergehäuse im SB-Ringraum [Calculation of H<sub>2</sub> Deflagration Loads to the Vent Filter Casing in the Annular Compartment of a Containment] , Final report BF-V68.391, Eschborn, 1997.
- [6.17] R. Hüper (Ed), Projekt Nukleare Sicherheitsforschung, Jahresbericht 1995, [Project of Nuclear Safety Research, Yearly Report 1995]; Report FZKA 5780, August 1996, 14.
- [6.18] E.Studer and M. Petit, Use of RUT Large Scale Combustion Test Results for Reactor Applications", SMIRT-14, Lyon, France, August 17-22, 1997.
- [6.19] B.E. Gelfand, S.P. Medvedev and B.E. Popov, Flame Stabilization and Flammability Limits of H<sub>2</sub>+air+steam (fog) Mixtures, Final report to FZK, contract 15/20089955/INR, December 1998